AN ISOBAR MODEL OF NUCLEON COMPTON SCATTERING

Thesis by

Robert William Weinman

In Partial Fulfillment of the Requirements

For the Degree of

Doctor of Philosophy

California Institute of Technology

Pasadena, California

1967

(Submitted 10 August 1966)

ACKNOWLEDGMENTS

The author wishes to thank Professor Jon Mathews for introducing him to the subject of Compton scattering and for his interest and help in seeing this thesis through to its conclusion.

He also wishes to thank Professor Robert Walker for providing him with much needed data on photoproduction, and Dr. D. Beder for many fruitful discussions. The author is indebted to Dr. Egon Marx and Mr. Thomas Nagylaki for helpful conversations.

Finally, the author wishes to thank the National Science Foundation for the predoctoral fellowship which was awarded to him during part of the time that the work on this thesis was being undertaken.

ABSTRACT

The Compton scattering of photons by nucleons is described in terms of an isobar model for the resonant states, using a spin 3/2 propagator and couplings at the vertices obtained from a phenomenological analysis of pion photo-production. The full Born term is taken into account, as well as contributions from pi and eta exchange in the t-channel.

Numerical results are obtained at 90^{o} in the center of mass system for the energy range 300 to 800 MeV which agree substantially with experiment. The recoil nucleon polarization and the cross-sections for polarized photons are also calculated over this energy range.

TABLE OF CONTENTS

	Page
ACKNOWLEDGMENTS	ii
ABSTRACT	iii
CHAPTER	
I. Introduction	1
II. Kinematics	5
III. Isobar Contributions	15
IV. Born Term Contribution	31
V. Low Amplitudes	35
VI. Calculation of Cross-Sections and Comparison with Experiment	39
VII. Discussion	42
APPENDICES	
I. Transformations between Amplitudes	46
II. Spin 5/2 Propagator	51
III. Table of Matrix Elements between Helicity States	52
IV. Shifting of Resonant Peaks	53
V. Multipole Analysis	54
TABLES	61
FIGURES	69
GRAPHS	71
REFERENCES	76

I. INTRODUCTION

The scattering of light by nucleons has been investigated for the last twelve years by both theoreticians and experimentalists. At low energies, that is, for energies below that of the first resonant peak, Compton scattering has afforded one of the most successful applications of dispersion relations and the unitarity of the S-matrix[1]. When it became clear that the absorbtive part of the amplitude, due to pion photoproduction, was responsible for the large increase in the cross-section with energy, that was incorporated into the dispersion theory with good agreement up to 250 MeV[2]. Using these dispersion relations, Jacob and Mathews[3] took into account the contribution due to the exchange of a π^0 meson in the t-channel (known as the Low amplitude) and obtained a more detailed agreement with experiment in this sub-resonance region. Contogouris[4,5] used dispersion relations, on the basis of better data on photoproduction, to extend the theoretical analysis beyond the position of the first resonance. In doing so he found it necessary to introduce a small amount of electric quadrupole to the photoproduction amplitude in addition to the magnetic dipole amplitude used by Mathews[2]. He also included a contribution in the form of an electric dipole amplitude from the second resonance in photoproduction. His results agreed with experiment up to the resonance but were less successful at the peak and beyond it.

Hearn and Leader[6] used the Mandelstam representation to

derive fixed-angle dispersion relations and found that all the subtractions they needed could be gotten by applying the low-energy limit theorem of Gell-Mann and Goldberger[7]. They included the Low amplitude in their analysis but also found it necessary to add a constant s-wave contribution up to 600 MeV and a slowly varying p-wave contribution for energies above 500 MeV. Their resulting dispersion relations are quite complicated and based on some preliminary calculations[8] resulted in agreement up to the resonance, but, like Contogouris, less agreement beyond it. Holliday also used the Mandelstam representation but not including any effect of the second resonance got poor agreement above 200 MeV[9]. Owing to a controversy over the sign of the Low amplitude (to be discussed in Chapter V), Contogouris and Verganelakis[10] considered the effect of a t-channel η exchange on the cross-section for energies below 250 MeV.

More recent experiments have extended our knowledge of Compton scattering beyond the energies which these theoretical analyses describe well[11,12]. It is therefore interesting to develop a model which can successfully describe these results at higher energies. Such a model has been used by Salin and Gourdin[13,14,15] to describe pion photoproduction. They have represented the various pion-nucleon resonances as nucleon isobars of definite spin and isospin and with a complex mass, the real part of which corresponds to the observed positions of the pi-nucleon resonances and the imaginary part of which corresponds to their observed widths. Using

the appropriate Feynman diagrams they calculate pion photoproduction cross-sections by means of propagators appropriate to particles of spin 3/2 which have suitable couplings at the vertices γN and πN. By fitting their result to the observed cross-section they obtain values for the coupling constants at the vertices. There are two of these at each vertex where an isobar couples to a nucleon and a photon and one at the vertex where an isobar couples to a nucleon and a pion. This latter coupling is found from a similar consideration of pi-nucleon scattering.

In this thesis we shall calculate Compton cross-sections using this model, known as the isobar model. We shall represent the total amplitude as a sum of Feynman diagrams pictured in Figure 2:

(A) Born amplitude, arising from a single nucleon intermediate state (N).

(B) Crossed Born term (N)

(C) First resonance amplitude (N*).

(D) Second resonance amplitude (N**).

(E) Low amplitude for π^0 exchange.

(F) Low amplitude for η exchange.

We shall not include contributions from higher pion-nucleon resonances because in the energy range (300 - 800 MeV) we shall be considering they are negligible. Also, we have not included any 2π contributions as they appear to be small[10].

In Chapter II the kinematics of Compton scattering is developed, including the propagators for higher spin and cross-

sections for unpolarized particles and for polarized particles. Chapter III will consider the isobar contributions, Chapter IV the Born term contribution and Chapter V the Low amplitudes. Chapter VI will compare results of our calculations with experiment and Chapter VII will discuss these results.

II. KINEMATICS

A. Preliminaries

We consider the process

$$\gamma_1 + N_1 \longrightarrow \gamma_2 + N_2 \tag{2.1}$$

where γ_1 is a photon of momentum k_1 and polarization ϵ_1 which is scattered off a nucleon N_1 of momentum p_1 to produce a photon γ_2 of momentum k_2 (and polarization ϵ_2) and a nucleon of momentum p_2.

It is often convenient to use the quantities

$$\begin{aligned} s &= -(p_1 + k_1)^2 \\ t &= -(p_1 - p_2)^2 \\ u &= -(p_1 - k_2)^2 \end{aligned} \tag{2.2}$$

where it follows that

$$s + t + u = 2M^2 \tag{2.3}$$

where M is the nucleon mass.

Calling the process described in (2.1), Channel I, we will also consider the processes of Channels II and III

$$\gamma_2 + N_1 \longrightarrow \gamma_1 + N_2 \quad \text{(Channel II)} \tag{2.4}$$

$$N_1 + \bar{N}_2 \longrightarrow \gamma_1 + \gamma_2 \quad \text{(Channel III)} \tag{2.5}$$

where $\bar{N}_2$ represents an antinucleon.

In the center-of-mass system for Channel I, pictured in Figure 1, we consider the nucleon N to have a four-momentum p_1 given by

$$p_1 = [0, 0, -p; (p^2 + M^2)^{1/2}] \tag{2.6}$$

where p is the magnitude of the nucleon 3-momentum, so that the photon, in the center-of-mass system for Channel I has four-momentum,

$$k_1 = [0, 0, p; p] \tag{2.7}$$

If the center-of-mass scattering angle is θ it follows that

$$\begin{aligned} p_2 &= [-p \sin\theta, 0, -p\cos\theta; (p^2+M^2)^{1/2}] \\ k_2 &= [+p \sin\theta, 0, +p\cos\theta; p] \end{aligned} \tag{2.8}$$

Substituting (2.6), (2.7), and (2.8) in (2.2) we find in thecenter-of-mass system of Channel I

$$\begin{aligned} s &= [p + (p^2+M^2)^{1/2}]^2 = (p+E)^2 = W^2 \\ t &= -2p^2(1-\cos\theta) \\ u &= -2p^2(1+\cos\theta) + [(p^2+M^2)^{1/2} - p]^2 \end{aligned} \tag{2.9}$$

where E is the total energy of the nucleon, $E = (M^2 + p^2)^{1/2}$, and W is the total center-of-mass energy of the nucleon and the photon. From (2.9) we see that

$$\begin{aligned} W^2 - M^2 &= 2Wp \\ W^2 + M^2 &= 2WE \end{aligned} \tag{2.10}$$

and since experimental results are given as a function of the laboratory photon energy we will need

$$W^2 - M^2 = 2 M k_{LAB} \tag{2.11}$$

where k_{lab} is the momentum of the photon in the laboratory which scatters off a nucleon initially at rest.

The S-matrix for the process may be written

$$S = 1 + i R \tag{2.12}$$

where R may be given in terms of the Feynman amplitude F,

$$R = \frac{M}{(2\pi)^2} (4 p_{10} p_{20} k_{10} k_{20})^{-1/2} \delta(p_1 - p_2 + k_1 - k_2) F \tag{2.13}$$

In each of the channels we can write the Feynman amplitude in terms of the spinors and polarization vectors of the initial and final nucleons and photons; the subscripts 1 and 2 refer, as before, to initial and final states

$$\begin{aligned} \langle \gamma_2 N_2 | F | \gamma_1 N_1 \rangle &= \epsilon^{\dagger}_{2\nu} \bar{u}_2(p_2) F_{\mu\nu} u_1(p_1) \epsilon_{1\mu} \\ \langle \gamma_1 N_2 | F | \gamma_2 N_1 \rangle &= \epsilon^{\dagger}_{1\nu} \bar{u}_2(p_2) F_{\mu\nu} u_1(p_1) \epsilon_{2\mu} \\ \langle \gamma_1 \gamma_2 | F | N_1 \bar{N}_2 \rangle &= \epsilon^{\dagger}_{2\nu} \bar{v}_2(-p_2) F_{\mu\nu} u_1(p_1) \epsilon^{\dagger}_{1\mu} \end{aligned} \tag{2.14}$$

The spinors u_1 and u_2 satisfy the Dirac equations

$$(i \gamma \cdot p_1 + M) u_1(p_1) = 0$$

$$(i\gamma\cdot p_2 + M)\, u_2(p_2) = 0 \qquad (2.15)$$

Since the nucleon has two possible spin states and the photon has two possible polarization states it would seem that there would be 2 x 2 initial states and 2 x 2 final states making a total of 16 possible independent amplitudes. However, consideration of symmetry under time reversal and space reflection reduces the number of independent amplitudes to 6. The function $F_{\mu\nu}$ in (2.14) has been decomposed into many different sets of invariant amplitudes by different authors, at first in terms of Pauli spinors[3,4] and later in terms of Dirac spinors with requirements that the amplitudes be free of kinematical singularities for use in dispersion relations[6,9]. In what follows we shall use the helicity amplitudes as developed by Jacob and Wick[16]. Since, for purposes of comparison of our results with other authors, it may be necessary to transform into other sets of amplitudes we have included in Appendix I the equations relating our amplitudes to several other sets.

Following the formalism of Jacob and Wick we define

$$\phi_i = \langle \lambda_{N_2}\, \lambda_{\gamma_2} \mid T \mid \lambda_{N_1}\, \lambda_{\gamma_1} \rangle \qquad (2.16)$$

$i = 1 \ldots 6$

where

$$T = \frac{M}{4\pi W} F \qquad (2.17)$$

and λN_2, $\lambda\gamma_2$, λN_1, $\lambda\gamma_1$ are the helicities of each of the particles,

helicity being defined as the projection of the spin of the particle along its direction of motion, $\lambda = \sigma \cdot \vec{p}/|\vec{p}|$. Thus for the nucleon we have $\lambda N = \pm \frac{1}{2}$ and $\lambda\gamma = \pm 1$ leading to 16 amplitudes of which 6 are independent. We shall choose as the 6 independent helicity amplitudes

$$\begin{aligned}
\phi_1 &= \langle \tfrac{1}{2} \; 1 | T | \tfrac{1}{2} \; 1 \rangle \\
\phi_2 &= \langle -\tfrac{1}{2} \; -1 | T | \tfrac{1}{2} \; 1 \rangle \\
\phi_3 &= \langle \tfrac{1}{2} \; -1 | T | \tfrac{1}{2} \; 1 \rangle \\
\phi_4 &= \langle -\tfrac{1}{2} \; 1 | T | \tfrac{1}{2} \; 1 \rangle \\
\phi_5 &= \langle \tfrac{1}{2} \; -1 | T | \tfrac{1}{2} \; -1 \rangle \\
\phi_6 &= \langle -\tfrac{1}{2} \; 1 | T | \tfrac{1}{2} \; -1 \rangle
\end{aligned} \tag{2.18}$$

In Table I are given the remaining helicity amplitudes in terms of these 6, obtained from considerations of symmetry under time reversal and space reflection.

B. Cross-Sections

In terms of the scattering amplitude T, the differential cross-section $\gamma_1 + N_1 \to \gamma_2 + N_2$ is given by

$$\frac{d\sigma}{d\Omega} = \sum |\langle \gamma_2 N_2 | T | \gamma_1 N_1 \rangle|^2 \tag{2.19}$$

where $\sum$ in the case of unpolarized particles means we are to average over the initial spins and polarizations and sum over the

final spins and polarizations. In terms of the helicity amplitudes we have then, for unpolarized particles

$$\frac{d\sigma}{d\Omega} = \frac{1}{2}\left[\phi_1^2 + 2\phi_3^2 + \phi_5^2 + \phi_2^2 + 2\phi_4^2 + \phi_6^2 \right] \qquad (2.20)$$

The simplicity of this expression for the cross-section is one of the advantages of using helicity amplitudes. There are no "hidden" energy or angular factors, as there are for the other amplitudes which have been used, for which the expressions for the cross-section contain energy and angular dependent factors.

Recently, it has become experimentally feasible to produce enough polarized photons to be able to measure separately the cross-sections for photons polarized either parallel or perpendicular to the plane of scattering[17]. It is therefore interesting to compute differential cross-sections for polarized photons.

We define the polarization four-vectors for photons of definite helicity traveling in the + z direction

$$\begin{aligned} \varepsilon_\mu^- &= +\frac{1}{\sqrt{2}}(1, -i, 0; 0) \\ \varepsilon_\mu^+ &= +\frac{1}{\sqrt{2}}(-1, -i, 0; 0) \end{aligned} \qquad (2.21)$$

corresponding to left-handed and right-handed circular polarization. Therefore, a photon traveling in the + z direction and polarized in the x direction (parallel to the scattering plane) is described by

$$\varepsilon_{\mu\,//} = -\frac{\sqrt{2}}{2}(\varepsilon_\mu^+ - \varepsilon_\mu^-) \qquad (2.22)$$

and a photon polarized in the y direction (perpendicular to the plane of scattering) by

$$\varepsilon_{\mu\perp} = +i\frac{\sqrt{2}}{2}\left(\varepsilon_{\mu}^{+} + \varepsilon_{\mu}^{-}\right) \tag{2.23}$$

Then we have for the T matrix elements for scattering from an initial photon state $\epsilon_\perp$ or $\epsilon_\parallel$ (nucleon spin indices are suppressed),

$$\begin{aligned}
\langle \alpha' | T | \epsilon_{\parallel} \rangle &= -\frac{\sqrt{2}}{2}\left[\langle \alpha' | T | + \rangle - \langle \alpha' | T | - \rangle\right] \\
\langle \alpha' | T | \varepsilon_{\perp} \rangle &= +i\frac{\sqrt{2}}{2}\left[\langle \alpha' | T | + \rangle + \langle \alpha' | T | - \rangle\right]
\end{aligned} \tag{2.24}$$

Calculating now the cross-sections,

$$\frac{d\sigma_\perp}{d\Omega} = \frac{1}{2}\sum_{\alpha'\beta'\beta} \langle \alpha'\beta' | T | \varepsilon_\perp \beta \rangle^{*} \langle \alpha'\beta' | T | \varepsilon_\perp \beta \rangle \tag{2.25}$$

where β,β' are the nucleon spin indices which we average over the initial state and sum over the final state as before, and we sum over the final helicity α',

$$\begin{aligned}
\frac{d\sigma_\perp}{d\Omega} = \frac{1}{2}\Big[&|\phi_1 + \phi_3|^2 + |\phi_4 + \phi_6|^2 \\
&|\phi_3 + \phi_5|^2 + |\phi_2 + \phi_4|^2 \Big]
\end{aligned} \tag{2.26}$$

which, using (2.20) may be written in the form

$$\frac{d\sigma_\perp}{d\Omega} = \left.\frac{d\sigma}{d\Omega}\right|_{\text{UNPOLARIZED}} + \mathrm{Re}\left[\phi_3^{*}(\phi_1 + \phi_5) + \phi_4^{*}(\phi_2 + \phi_6)\right] \tag{2.27}$$

Similarly for $\frac{d\sigma_\parallel}{d\Omega}$,

$$\frac{d\sigma_{\parallel}}{d\Omega} = \frac{1}{2}\left[|\phi_1 - \phi_3|^2 + |\phi_4 - \phi_6|^2 + |\phi_3 - \phi_5|^2 + |\phi_2 - \phi_4|^2\right] \quad (2.28)$$

which may be written

$$\frac{d\sigma_{\parallel}}{d\Omega} = \left.\frac{d\sigma}{d\Omega}\right|_{UNPOLARIZED} - Re\left[\phi_3^*(\phi_1 + \phi_5) + \phi_4^*(\phi_2 + \phi_6)\right] \quad (2.29)$$

From (2.27) and (2.29) we see immediately that

$$\left.\frac{d\sigma}{d\Omega}\right|_{UNP.} = \frac{1}{2}\left[\frac{d\sigma_{\perp}}{d\Omega} + \frac{d\sigma_{\parallel}}{d\Omega}\right] \quad (2.30)$$

as expected.

Another possible quantity which has recently become possible to measure experimentally is the polarization of the recoil nucleon, in the direction perpendicular to the scattering plane. Calling this quantity P, and defining P to be positive if the final state nucleon is polarized in the direction $\vec{k}_1 \times \vec{k}_2$, we obtain

$$P = \frac{Im\left[\phi_3^*(\phi_2 + \phi_6) + (\phi_1 + \phi_5)^* \phi_4\right]}{\left.\frac{d\sigma}{d\Omega}\right|_{UNP.}} \quad (2.31)$$

where only terms involving the product of amplitudes in which the spin of the nucleon changes with amplitudes in which the spin does not change occur. We notice that in (2.29) no such terms occur.

C. Higher Spin Propagators

In order to evaluate matrix elements for the N* and N** we will have to use the propagator for a particle with spin 3/2. We

shall use the Rarita-Schwinger formalism[18] for particles of arbitrary spin and represent the particle with a wavefunction ψ_ν which satisfies the wave equation

$$(\gamma_\mu \partial_\mu + M)\psi_\nu = 0 \tag{2.32}$$

with M being the mass of the particle. The wavefunction is subject to the conditions

$$\gamma_\mu \psi_\mu = 0 \qquad\qquad \partial_\mu \psi_\mu = 0 \tag{2.33}$$

The propagator may be determined in a number of ways, the simplest seems to be to write down an expression involving P_μ (the particle's four-momentum) and γ matrices of the most general form, with arbitrary coefficients,

$$P_{\mu\nu} = A\delta_{\mu\nu} + B\gamma_\mu\gamma_\nu + C(\gamma_\mu P_\nu - \gamma_\nu P_\mu) + D P_\mu P_\nu \tag{2.34}$$

and using (2.33), require that

$$\gamma_\mu P_{\mu\nu} = 0 \qquad\qquad P_\mu P_{\mu\nu} = 0 \tag{2.35}$$

in order to obtain the coefficients A, B, C, D. This will determine the propagator $P_{\mu\nu}$ apart from the question of normalization and this is obtained by requiring

$$\sum_{\text{SPINS}} \psi_\mu \bar{\psi}_\nu = -2M \tag{2.35a}$$

in the rest frame where it is easy to evaluate. The result for spin 3/2 is

$$P_{\mu\nu} = \frac{M - i\not{p}}{M^2 + p^2}\left[\delta_{\mu\nu} - \frac{1}{3}\gamma_\mu\gamma_\nu + \right.$$

$$\left. + \frac{i}{3M}(\gamma_\mu p_\nu - \gamma_\nu p_\mu) + \frac{2}{3M^2} p_\mu p_\nu \right] \qquad (2.36)$$

which agrees with the propagator used in (13).

Using this method we have also calculated the propagator for a spin 5/2 particle and the result will be found in Appendix II. We shall not use this result here but if one wanted to take into account the third pion-nucleon resonance which has spin 5/2, this propagator could be used. Its complexity, however, would seem to preclude its utility.

III. ISOBAR CONTRIBUTIONS

In the isobar model, as used by Salin and Gourdin in their analysis of photoproduction[13,14,15] we consider the diagrams illustrated in Figures 2C and 2D and calculate their contribution to the amplitude by the usual Feynman rules. We use for the N* and N** propagators the spin 3/2 propagator derived in Chapter II and take into account the fact that these are actually not particles of definite mass but are resonances of the pion-nucleon system located at some energy M_R in the center-of-mass system and with a phenomenological width Γ.

A. First Resonance (N*)

At the N N* γ vertex we have an interaction Hamiltonian

$$H_{NN^*\gamma} = H_3 + H_4 + H_5 \tag{3.1}$$

with H_3, H_4 and H_5 given by

$$\begin{aligned}
H_3 &= -\frac{eC_3}{m_\pi}\left[\bar{\psi}_N \gamma_\mu\gamma_5 \psi_\nu + \bar{\psi}_\nu \gamma_5\gamma_\mu \psi_N\right] F_{\mu\nu} \\
H_4 &= -\frac{eC_4}{m_\pi^2}\left[\bar{\psi}_N \gamma_5 \frac{\partial}{\partial x_\mu}\psi_\nu + \frac{\partial}{\partial x_\mu}\bar{\psi}_\nu \gamma_5 \psi_N\right] F_{\mu\nu} \\
H_5 &= +\frac{eC_5}{m_\pi^2}\left[\frac{\partial}{\partial x_\mu}\bar{\psi}_N \gamma_5 \psi_\nu + \bar{\psi}_\nu \gamma_5 \frac{\partial}{\partial x_\mu}\psi_N\right] F_{\mu\nu}
\end{aligned} \tag{3.2}$$

where ψ_N is the wavefunction of the nucleon, ψ_ν is the wavefunction for the N*, m_π is the pion mass, e is the electric charge and $F_{\mu\nu}$ is

the electromagnetic field tensor

$$F_{\mu\nu} = \frac{\partial A_\mu}{\partial x_\nu} - \frac{\partial A_\nu}{\partial x_\mu} \tag{3.3}$$

which makes the Hamiltonian gauge invariant.

Since for Compton scattering the photon is a free particle, it follows that $H_4 = H_5$ so that for Compton scattering we have

$$H_{NN^*\gamma} = H_3 + 2H_5 \tag{3.4}$$

and there are just two constants needed to describe the interaction. This is analogous to the NNγ coupling where two constants F_1 and F_2 are needed (see Chapter IV). Any other type of coupling can be shown to reduce to some linear combination of these, upon application of the condition

$$\frac{\partial F_{\mu\nu}}{\partial x_\mu} = 0 \tag{3.5}$$

In the case of electroproduction, where the photon is a virtual particle it would be necessary to include both H_4 and H_5.

The constants C_3 and C_5 are determined by analysis of photoproduction data. This was done by Salin and Gourdin who used[13,14,15] this model to make a phenomenological fit and they found

$$\begin{aligned} C_3 &= 0.37 \\ C_5 &= -0.0043 \end{aligned} \tag{3.6}$$

using a phenomenological width in the laboratory system of 160 MeV. With these parameters they are able to fit the photoproduction data very well up to 500 MeV including such features as the correct

shifting of the maximum to lower energy due to interference of the isobar with the background and the angular distribution of the differential cross-section. Also the constants they obtain from π^0 photoproduction data agree with those obtained from π^+ photoproduction data. Their analysis was less successful with increasing energy because beyond the first resonance the second resonance plays an increasingly important role and we have reason to believe that their analysis of the second resonance is not correct. This will be discussed in part B of this Chapter.

In addition to the fitting of photoproduction, the isobar model of Salin and Gourdin, using these values for the constants, has been applied[19] to electroproduction where the pion producing photon is virtually produced in the scattering of an electron by a nucleon Here we must, as pointed out previously, retain the H_4 term independently in 3.1 and three parameters are needed. However, the constants C_3 and C_5 were used to obtain a good fit.

Mathews, in discussing the decay of the Ω^- [20] has used values somewhat different than those used here. By considering detailed balancing he relates the area under the total cross-section curve to the magnetic dipole width in photoproduction, and also to the total width times the cross-section at maximum assuming a Breit-Wigner form for the total cross-section curve. He then assumes that the resonance is pure magnetic dipole, setting $\Gamma_{E2} = 0$, and obtains

$$C_3 = \frac{C_{3(Mathews)} \times m_\pi}{1\ BeV} = 0.30$$

$$C_5 = \frac{1}{2}\frac{C_{5(Mathews)} \times m_\pi^2}{1\ BeV^2} = -0.017 \qquad (3.7)$$

Even allowing for a discrepancy in the widths used, there still remains a difference in these two results. (Mathews uses a center-of-mass width of 110 MeV while Salin and Gourdin a laboratory width of 160 MeV corresponding to a center-of-mass width of 120 MeV but this only increases the Mathews result to 0.33 as opposed to S & G's 0.38.) The difference may be due to the assumption of a Breit-Wigner form of Mathews and we have chosen to use the Salin and Gourdin result, for the reasons cited above. The discrepancy in C_5 is more understandable and is due to the sensitivity with which C_5 depends on the ratio of the electric quadrupole to the magnetic dipole amplitudes. In obtaining C_5, Mathews sets this ratio equal to 0 while Salin and Gourdin find it necessary to have this ratio ρ equal to .045. From

$$\frac{C_5(\rho)}{C_5(\rho=0)} \approx 1 - \rho\left[\frac{4M_R}{M_R - M}\right] \approx 1 - 16\rho \qquad (3.7a)$$

we see that a 4.5 percent admixture of electric quadrupole leads to $C_5 = (-.017)(.28) = -.0048$ which agrees with Salin and Gourdin.

We now proceed to evaluate the N* contribution using the interaction Hamiltonians H_3 and H_5. Using primes to denote final states and unprimed quantities initial states we have

$$H^\dagger H = H_3^\dagger H_3 + 4 H_5^\dagger H_5 + 2\left(H_3^\dagger H_5 + H_5^\dagger H_3\right) \tag{3.8}$$

and substituting from (3.2)

$$H_3^\dagger H_3 = \frac{e^2 C_3^2}{m_\pi^2}\left[F^{*\prime}_{\beta\mu}\,\bar\psi_{N'}\,\gamma_\beta\,\gamma_5\,\psi'_\mu\,\bar\psi_\nu\,\gamma_5\,\psi_N\,F_{\alpha\nu}\,\gamma_\alpha\right]$$

$$H_3^\dagger H_3 = \frac{e^2 C_3^2}{m_\pi^2}\left[F^{*\prime}_{\beta\mu}\,\bar\psi_{N'}\,\gamma_5\,\gamma_\beta\,\mathbb{P}_{\mu\nu}\,\gamma_\alpha\,\gamma_5\,\psi_N\,F_{\alpha\nu}\right] \tag{3.9}$$

where $\mathbb{P}_{\mu\nu}$ is the propagator (2.36). Writing $A_\nu = \epsilon_\nu\, e^{ik_\alpha x_\alpha}$ where ϵ_ν is the photon polarization four vector and k_α the four momentum we have $\gamma_\alpha F_{\alpha\nu} = i\,(\not{\epsilon}\, k_\nu - \not{k}\,\epsilon_\nu)$ and

$$H_3^\dagger H_3 = \frac{e^2 C_3^2}{m_\pi^2}\left[\bar u_f\,(\not{\epsilon}'\,k'_\mu - \not{k}'\,\epsilon'_\mu)^*\,\gamma_5\,\mathbb{P}_{\mu\nu}\,\gamma_5\,(\not{\epsilon}\,k_\nu - \not{k}\,\epsilon_\nu)\,u_i\right] \tag{3.10}$$

where u_f and u_i are the final and initial nucleon Dirac spinors of momentum p'_α, p_α.

Similarly,

$$4\,H_5^\dagger H_5 = \frac{4e^2 C_5^2}{m_\pi^4}\Big[\bar\psi_{N'}\,p'_\beta\,(\epsilon'_\beta k'_\mu - k'_\beta \epsilon'_\mu)^* \times \gamma_5\,\mathbb{P}_{\mu\nu}\,\gamma_5\,(\epsilon_\alpha k_\nu - k_\alpha \epsilon_\nu)\,p_\alpha\,\psi_N\Big] \tag{3.11}$$

$$4\,H_5^\dagger H_5 = \frac{4e^2 C_5^2}{m_\pi^4}\Big[\bar u_f\,(p'\cdot\epsilon'\,k'_\mu - p'\cdot k'\,\epsilon'_\mu)^* \times \gamma_5\,\mathbb{P}_{\mu\nu}\,\gamma_5\,(p\cdot\epsilon\,k_\nu - p\cdot k\,\epsilon_\nu)\,u_i\Big] \tag{3.12}$$

and

$$2\left(H_5^\dagger H_3 + H_3^\dagger H_5\right) = \frac{-2e^2 C_3 C_5}{m_\pi^3}\left[-F^{*\prime}_{\alpha\mu}\bar{\psi}_{N'} p'_\alpha \gamma_5 \times \mathbb{P}_{\mu\nu}\gamma_5 \psi_N F_{\beta\nu}\gamma_\beta + F^{*\prime}_{\alpha\mu}\bar{\psi}'_N \gamma_\alpha \gamma_5 \mathbb{P}_{\mu\nu}\gamma_5 p_\beta \psi_N F_{\beta\nu}\right] \tag{3.13}$$

If we define

$$\begin{aligned} A_\mu &= \not{\varepsilon} k_\mu - \not{k}\varepsilon_\mu \\ B_\mu &= (p\cdot\varepsilon)k_\mu - (p\cdot k)\varepsilon_\mu \\ \gamma_5 \mathbb{P}_{\mu\nu}\gamma_5 &= \bar{\bar{\mathbb{P}}}_{\mu\nu} \end{aligned} \tag{3.14}$$

then

$$H^\dagger H = \bar{u}_f\left[\frac{e^2 C_3^{\,2}}{m_\pi^2} A'_\mu \bar{\bar{\mathbb{P}}}_{\mu\nu} A_\nu + \frac{4e^2 C_5^{\,2}}{m_\pi^4} B'_\mu \bar{\bar{\mathbb{P}}}_{\mu\nu} B_\nu + \frac{2i e^2 C_3 C_5}{m_\pi^3}\left(B'_\mu \bar{\bar{\mathbb{P}}}_{\mu\nu} A_\nu - A'_\mu \bar{\bar{\mathbb{P}}}_{\mu\nu} B_\nu\right)\right] u_i \tag{3.15}$$

and we define M by

$$H^\dagger H = \bar{u}_f M u_i \tag{3.15a}$$

We will evaluate this in the center-of-mass system, choosing coordinates so that

$$k_\mu = (0, 0, k\,;\ k)$$
$$p_\mu = (0, 0, -k\,;\ (k^2+M^2)^{1/2})$$
$$\varepsilon = (\vec{\varepsilon}, 0)$$
$$\varepsilon' = (\vec{\varepsilon}', 0)$$

so

$$p\cdot\varepsilon = k\cdot\varepsilon = 0$$
$$k_\mu p_\mu = \vec{k}\cdot\vec{p} - k_0 p_0$$
$$A_\mu = \not{k}\, k_\mu - \not{k}\, \varepsilon_\mu$$
$$B_\mu = k W \varepsilon_\mu \qquad (3.16)$$

Substituting (3.16) into (3.15) leads to

$$M = a^2 \bar{A}_\mu \bar{\bar{P}}_{\mu\nu} A_\nu + b^2 k^2 W^2 \varepsilon^*_\mu \bar{\bar{P}}_{\mu\nu} \varepsilon_\nu +$$
$$+ ab\, kW i (\varepsilon^*_\mu \bar{\bar{P}}_{\mu\nu} A_\nu - \bar{A}_\mu \bar{\bar{P}}_{\mu\nu} \varepsilon_\nu) \qquad (3.17)$$

where * is a complex conjugation. We define the quantities

$$a = \frac{e C_3}{m_\pi} \qquad b = \frac{2e C_5}{m_\pi^2} \qquad (3.18)$$

Substituting (2.36) in (3.17), replacing the denominator by its value in the center-of-mass system, using M_R in place of M for the mass of the isobar, and inserting the phenomenological width Γ

$$M^2 + P^2 \longrightarrow M_R^2 - W^2 - i M_R \Gamma \equiv \Delta^2 \qquad (3.19)$$

we obtain after some algebra

$$\begin{aligned}
\Delta^2 \bar{A}_\mu \bar{\bar{P}}_{\mu\nu} A_\nu = {} & 2\left[(-M_R W E - W^2 M)\, \varepsilon' \cdot \varepsilon \right] 1 \\
& + 2\left[(M_R W M + W^2 E)\, \varepsilon' \cdot \varepsilon \right] \beta \\
& + \left[(M M_R + W^2)\, k \cdot \varepsilon' \right] i \not{\varepsilon} \\
& + \left[(M M_R + W^2)\, k' \cdot \varepsilon \right] i \not{\varepsilon}' \\
& + \left[(-WM - W M_R)\, k \cdot \varepsilon' \right] i \beta \not{\varepsilon} \\
& + \left[(-WM - W M_R)\, k' \cdot \varepsilon \right] i \not{\varepsilon}' \beta \\
& + \left[M_R\, k' \cdot k + \tfrac{8}{3} W E M_R + \tfrac{8}{3} W E M - \tfrac{4}{3} \frac{W^2 k E}{M_R} + \tfrac{4}{3} W k M \right] \not{\varepsilon}' \not{\varepsilon} \\
& + \left[W\, k' \cdot k - \tfrac{8}{3} W M M_R - \tfrac{8}{3} W M^2 + \tfrac{4}{3} \frac{W^2 k M}{M_R} - \tfrac{4}{3} W^2 k + \tfrac{2}{3} \frac{W^3 k^2}{M_R^2} \right] \beta \not{\varepsilon}' \not{\varepsilon}
\end{aligned} \qquad (3.20)$$

$$\begin{aligned}
\Delta^2 (\varepsilon^{*\prime}_\mu \bar{\bar{P}}_{\mu\nu} A_\nu - \bar{A}_\mu \bar{\bar{P}}_{\mu\nu} \varepsilon_\nu) = {} & \left[M_R\, k \cdot \varepsilon' \right] i \not{\varepsilon} \\
& + \left[M_R\, k' \cdot \varepsilon \right] i \not{\varepsilon}' \\
& + \left[-W\, k \cdot \varepsilon' \right] i \beta \not{\varepsilon} \\
& + \left[W\, k' \cdot \varepsilon \right] i \not{\varepsilon}' \beta
\end{aligned}$$

$$\begin{aligned}
\Delta^2 \varepsilon^{*\prime}_\mu \bar{\bar{P}}_{\mu\nu} \varepsilon_\nu = {} & \left[M_R\ \varepsilon' \cdot \varepsilon \right] 1 \\
& \left[-W\ \varepsilon' \cdot \varepsilon \right] \beta \\
& \left[-\tfrac{1}{3} M_R \cdot 1 \right] \not{\varepsilon}' \not{\varepsilon} \\
& \left[\tfrac{1}{3} W \cdot 1 \right] \beta \not{\varepsilon}' \not{\varepsilon}
\end{aligned}$$

Now we must sandwich M between spinors representing initial and final nucleon states and since we are using helicity amplitudes we must calculate the matrix elements of the Dirac matrices between helicity spinors. Since these may be of possible general use they are given in Appendix III.

The photons must also be represented in helicity eigenstates. There are two such states, corresponding to the two directions of circular polarization as previously noted. We have, as in (2.21) for a photon traveling in the + z direction

$$\begin{aligned} \varepsilon_\mu^+(0) &= \frac{-1}{\sqrt{2}}(1, i, 0; 0) \\ \varepsilon_\mu^-(0) &= \frac{+1}{\sqrt{2}}(1, -i, 0; 0) \end{aligned} \tag{3.21}$$

where the gauge is chosen so that fourth component of ϵ_μ is 0. For the final state we have a photon scattered by an angle θ from the initial photon and thus

$$\begin{aligned} \varepsilon'^{*+}_\mu(\theta) &= \frac{-1}{\sqrt{2}}(\cos\theta, -i, -\sin\theta; 0) \\ \varepsilon'^{*-}_\mu(\theta) &= \frac{+1}{\sqrt{2}}(\cos\theta, +i, -\sin\theta; 0) \end{aligned} \tag{3.22}$$

or leaving the helicity as a free index $\alpha = \pm 1$.

$$\begin{aligned} \varepsilon^\alpha_\mu(0) &= \frac{+1}{\sqrt{2}}(-\alpha, -i, 0; 0) \\ \varepsilon'^{*\alpha'}_\mu(\theta) &= \frac{1}{\sqrt{2}}(-\alpha\cos\theta, i, \alpha\sin\theta; 0) \end{aligned} \tag{3.23}$$

In this coordinate system

$$k = (0, 0, k; k)$$

$$k' = (k\sin\theta, 0, k\cos\theta; k)$$

so that

$$\begin{aligned} \varepsilon^{*\alpha'}\cdot\varepsilon^{\alpha} &= \tfrac{1}{2}(1+\alpha'\alpha\cos\theta) \\ \varepsilon^{*\alpha'}\cdot k &= \tfrac{1}{\sqrt{2}}(\alpha' k\sin\theta) \\ k'\cdot\varepsilon^{\alpha} &= \tfrac{1}{\sqrt{2}}(-\alpha k\sin\theta) \\ k'\cdot k &= k^2(\cos\theta-1) \end{aligned} \qquad (3.24)$$

Using Appendix III we obtain for $\bar{u}_f M u_i$ the contribution of the first isobar to the total amplitude

$$\bar{u}_f M u_i = \bar{u}_f\left[a^2 A' \bar{\bar{P}} A + b^2k^2W^2\,\varepsilon'\bar{\bar{P}}\varepsilon + abkW_i(\varepsilon'\bar{\bar{P}}A - A'\bar{\bar{P}}\varepsilon)\right]u_i$$

$$\bar{u}_f \Delta^2 A' \bar{\bar{P}} A u_i = \left\{ \begin{aligned} &\Big[W^2(1+\alpha'\alpha\cos\theta) + (W^2+MM_R)\Big(\frac{\alpha'+\alpha+2\alpha'\alpha}{2}\Big)(1-\cos\theta) \\ &\Big[WM_R(1+\alpha'\alpha\cos\theta) + (WM_R+MW)\Big(\frac{\alpha-\alpha'-2\alpha'\alpha}{2}\Big)(1+\cos\theta) \\ &\quad + (WE+MM_R)\frac{(\alpha'-1)(\alpha+1)}{2}(1-\cos\theta) \\ &\quad + (EM_R+MW)\frac{(1-\alpha')(1+\alpha)}{2}(1+\cos\theta) \\ &+ \frac{2}{3}\Big(\frac{W}{M_R}\Big)^2(WE-2M_R^2)\frac{(1+\alpha')(1+\alpha)}{2}\Big]\cos\frac{\theta}{2} \\ &+ \frac{2}{3}\Big(\frac{W}{M_R}\Big)\Big(W^2-\frac{W^2M}{M_R}-4M_R^2-2MM_R-M^2\Big)\frac{(1-\alpha')(1+\alpha)}{2}\Big]\sin\frac{\theta}{2} \end{aligned} \right\} \qquad (3.25$$

$$\bar{u}_f \Delta^2 \varepsilon' \bar{\bar{P}} \varepsilon u_i = \frac{1}{2M}\left\{ \begin{aligned} &(MM_R-WE)\Big(1+\alpha'\alpha\cos\theta-\frac{(1+\alpha')(1+\alpha)}{3}\Big)\cos\frac{\theta}{2} \\ &(MW-EM_R)\Big(1+\alpha'\alpha\cos\theta-\frac{(1-\alpha')(1+\alpha)}{3}\Big)\sin\frac{\theta}{2} \end{aligned} \right\}$$

$$\bar{u}_f \Delta^2 i \left(\varepsilon' \bar{\bar{P}} A - A' \bar{\bar{P}} \varepsilon\right)_{\mu_i} = \frac{k^2}{M} \begin{Bmatrix} M_R \left(\frac{\alpha' - \alpha}{2}\right)(1 - \cos\theta)\cos\frac{\theta}{2} \\ W \left(\frac{-\alpha' - \alpha}{2}\right)(1 + \cos\theta)\sin\frac{\theta}{2} \end{Bmatrix}$$

where $\Delta^2 = M_R^2 - W^2 - i M_R \Gamma$

W = total energy in center-of-mass system

k = photon momentum in center-of-mass system

θ = center-of-mass scattering angle

E = center-of-mass nucleon energy

M = nucleon mass

M_R = mass of N* isobar

α', α = final and initial photon helicities

$a = \frac{ec_3}{m\pi}$ $\quad b = \frac{2ec_5}{m_\pi 2}$

and the upper expression in each bracket is to be used when the nucleon helicity changes sign and the lower expressions when the helicity remains the same. This expression for M vanishes for k = 0 so the isobar does not contribute at all in the low energy limit. In Ref. (14) this k dependence was ignored and consequently their fit is not good in the very low energy range. Substituting appropriate values for α' and α we obtain the contribution to our 6 helicity amplitudes as a function of energy and scattering angle and tabulate the result of a numerical calculation at 90^o for different energies in Table II.

B. Second Resonance (N**)

We proceed as for the first resonance and write

$$H_{NN^{**}\gamma} = G_3 + G_4 + G_5 \tag{3.26}$$

However, since the parity of the N** is opposite to the parity of the N* we now have for the interaction Hamiltonians:

$$G_3 = \frac{-eD_3}{m_\pi}\left[\bar{\psi}_N \gamma_\mu \psi_\nu + \bar{\psi}_\nu \gamma_\mu \psi_N\right] F_{\mu\nu}$$

$$G_4 = \frac{-eD_4}{m_\pi^2}\left[\bar{\psi}_N \frac{\partial}{\partial x_\mu} \psi_\nu + \frac{\partial}{\partial x_\mu} \bar{\psi}_\nu \psi_N\right] F_{\mu\nu} \tag{3.27}$$

$$G_5 = \frac{eD_5}{m_\pi^2}\left[\frac{\partial}{\partial x_\mu} \bar{\psi}_N \psi_\nu + \bar{\psi}_\nu \frac{\partial}{\partial x_\mu} \psi_N\right] F_{\mu\nu}$$

As before, G_4 and G_5 are equivalent for a real photon and we may write

$$H_{NN^{**}\gamma} = G_3 + 2G_5 \tag{3.28}$$

For the coupling constants D_3 and D_5 we will not use the values given by Salin and Gourdin[15] for reasons given below, but will instead use the phenomenological analysis of Walker[22]) who from an analysis of pion photoproduction found

$$E_{2-} = -1.270 \qquad M_{2-} = -0.312 \tag{3.29}$$

To relate these results to the coupling constants which we will need to make use of the isobar analysis of photoproduction for the 2nd

resonance. Using the notation of (15) we have, with appropriate isospin factors,

$$M_{2-} = \frac{1}{2} L_2$$
$$E_{2-} = \frac{1}{2}(2L_1 - L_2) \tag{3.30}$$

where L_1 and L_2 are the numerator functions in the isobar analysis and are given by

$$L_1 = \frac{-2Wq^2}{E_2+M} \lambda_2 D_1 \frac{e}{\mu}$$
$$L_2 = \frac{-2Wk^2q^2}{(E_1+M)(E_2+M)} \lambda_2 D_2 \frac{e}{\mu^2} \tag{3.31}$$

where E_1 and E_2 are the initial and final nucleon energies, k and q are the photon and pion momenta, W is the center-of-mass total energy, λ_2 is the pion-nucleon-N* coupling constant found from pi-nucleon scattering to be 2.07, and μ is the pion mass. By this we can evaluate D_1 and D_2 which are the coupling constants using non-gauge-invariant Hamiltonians and by means of

$$D_3 = D_2$$
$$D_5 = D_4 = \frac{m_\pi^2}{W_R^2 - M^2} D_1 \left(1 - \frac{D_2}{D_1} \frac{W_R+M}{m_\pi}\right) \tag{3.32}$$

obtain D_4 and D_5. From (3.29) and (3.30) we have

$$L_1 = -1.58 \qquad L_2 = -0.62 \tag{3.33}$$

and from (3.31), evaluating the energy dependent part at the mass of the second resonance, we obtain

$$D_3 = -0.048$$

$$D_5 = +0.009$$

The reason for not using the second resonance parameters given by Salin and Gourdin is that they do not give the observed small cross-sections for forward angles in the second resonance region. This was first pointed out by Beder[21]. At 0^o, the photoproduction cross-section may be written

$$\left.\frac{d\sigma}{d\Omega}\right|_{0^o} = |\mathcal{F}_1 - \mathcal{F}_2|^2_{0^o} \tag{3.34}$$

If one looks at the contributions to the imaginary part of the amplitude at the position of the resonance one finds a large contribution only from the amplitude due to that resonance so we may write, at 0^o,

$$\begin{aligned} \mathcal{F}_1 &= E_{2-} + 3M_{2-} \\ \mathcal{F}_2 &= 0 + 6M_{2-} \end{aligned} \tag{3.35}$$

so that

$$\left.\frac{d\sigma}{d\Omega}\right|_{0^o} = |E_{2-} - 3M_{2-}|^2 \tag{3.36}$$

If one uses the parameters of Salin and Gourdin one obtains $E_{2-} \sim 1.4$ and $M_{2-} \sim 0$ so that

$$\left.\frac{d\sigma}{d\Omega}\right|_{0^\circ} \approx 2$$

while with parameters dictated by Walker's result and which are used here, one obtains

$$\left.\frac{d\sigma}{d\Omega}\right|_{0^\circ} \approx 0.1$$

which is 20 times smaller giving a forward angle cross-section of 0.1 μb as opposed to the 2 μb of Salin and Gourdin. Since 0.1 μb is about what is observed it seems more reasonable to use the Walker results.

We proceed now as for the first resonance and calculate the contribution to the amplitude from Figure 2D using the interactions defined in (3.27). We write

$$c = \frac{eD_3}{m_\pi} \qquad d = \frac{2eD_5}{m_\pi^2} \tag{3.37}$$

and we obtain the result

$$M = c^2 A' \bar{\bar{P}} A + d^2 k^2 W^2 \varepsilon' \bar{\bar{P}} \varepsilon + dc\, kW i(\varepsilon' \bar{\bar{P}} A - A' \bar{\bar{P}} \varepsilon)$$

$$\bar{u}_f \Delta^2 i(\varepsilon' \bar{\bar{P}} A - A' \bar{\bar{P}} \varepsilon) u_i = \frac{k^2}{M} \begin{Bmatrix} M_R\left(\frac{\alpha'-\alpha}{2}\right)(1-\cos\theta)\cos\frac{\theta}{2} \\ W\left(\frac{\alpha'+\alpha}{2}\right)(1+\cos\theta)\sin\frac{\theta}{2} \end{Bmatrix} \tag{3.38}$$

$$\bar{u}_f \Delta^2 \varepsilon' \bar{\bar{P}} \varepsilon u_i = \frac{1}{2M} \begin{Bmatrix} (WE + MM_R)\left(1 + \alpha'\alpha\cos\theta - \frac{(1+\alpha')(1+\alpha)}{3}\right)\cos\frac{\theta}{2} \\ (-M_R E - MW)\left(1 + \alpha'\alpha\cos\theta - \frac{(1-\alpha')(1+\alpha)}{3}\right)\sin\frac{\theta}{2} \end{Bmatrix}$$

$$\bar{u}_f \Delta^2 A' \bar{\bar{P}} A u_i = \frac{k^2}{M} \left\{ \begin{array}{l} \left[-W^2(1+\alpha'\alpha\cos\theta) + (W^2 - MM_R)\left(\frac{-\alpha'-\alpha-2\alpha'\alpha}{2}\right)(1-\cos\theta) \right. \\ \left[M_R W(1+\alpha'\alpha\cos\theta) + (-WM_R + MW)\left(\frac{\alpha'-\alpha+2\alpha'\alpha}{2}\right)(1+\cos\theta) \right. \end{array} \right.$$

$$+ (WE - MM_R)\left(\frac{(1+\alpha')(1+\alpha)}{2}\right)(1-\cos\theta)$$

$$+ (-EM_R + MW)\left(\frac{(\alpha'-1)(\alpha'+1)}{2}\right)(1+\cos\theta)$$

$$\left. \begin{array}{l} + \frac{2}{3}\left(\frac{W}{M_R}\right)^2 (2M_R^2 - WE)\left(\frac{(1+\alpha')(1+\alpha)}{2}\right)\Big] \cos\frac{\theta}{2} \\ + \frac{2}{3}\left(\frac{W}{M_R}\right)\left(-W^2 - \frac{W^2 M}{M_R} + 4M_R^2 - 2MM_R + M^2\right)\left(\frac{(\alpha'-1)(\alpha'+1)}{2}\right)\Big] \sin\frac{\theta}{2} \end{array} \right\}$$

where as before the upper expressions in the brackets are for non spin-flip and the lower expressions for spin flip amplitudes. Substituting for each of the six helicity amplitudes appropriate values of α', α we obtain the N** contribution as a function of energy and angle and have given in Table III the result at 90°.

In Table VIII is given a summary of the properties of the N* and N** including the interaction parameters which we have used.

IV. BORN TERM CONTRIBUTION

To calculate the contribution to the amplitude of the one-nucleon intermediate state diagrams, or Born term, (Figures 2A and 2B, the uncrossed and crossed diagrams) we use, at the γNN vertices the usual electric and magnetic form factors $F_1(k^2)$, $F_2(k^2)$, including the full proton anomalous magnetic moment. Since the photons in Compton scattering are real and not virtual we have $k^2 = 0$ so that we need only use the values of the form factors for $k^2 = 0$:

$$F_1 \equiv F_1(0) = e \qquad F_2 \equiv F_2(0) = \frac{\mu' e}{2M} \tag{4.1}$$

where μ' is the anomalous part of the proton magnetic moment. Then we have, at each vertex, the matrix element

$$\langle N | R | \gamma_1 N_1 \rangle = \langle p'' | R | k_1 p_1 \rangle =$$

$$\frac{-M}{2(\pi p_0'' p_{10} k_{10})^{1/2}} u(p'') \left[F_1 \gamma_\nu - F_2 \sigma_{\nu\mu} k_\mu \right] \varepsilon_{1\nu} u(p_1) \tag{4.2}$$

where p'' is the momentum of the intermediate nucleon and $\sigma_{\nu\mu} = \frac{1}{2}(\gamma_\nu\gamma_\mu - \gamma_\mu\gamma_\nu)$. With this, we evaluate the diagrams and adding them together obtain the full Born term

$$\frac{8\pi W \phi_1}{e^2 \kappa} = \left(\frac{M^2}{E^2} + \frac{\mu p}{E} \right)(1 - \cos\theta) + (\mu^2 - 1)\frac{E}{M} - (\mu^2 + 1)$$

$$\frac{8\pi W \phi_3}{e^2 \kappa} = \left(-\frac{M}{E} \right)(1 - \cos\theta) + (\mu^2 - 1)\left(\frac{W}{M} - \frac{2p}{E} - 1 \right)$$

$$\frac{8\pi W\phi_5}{e^2 c} = \left(\frac{M^2}{E^2} - \frac{\mu p}{E}\right)(1-\cos\theta) + (\mu^2-1)\frac{E}{M} - (\mu^2+1)$$

$$\frac{8\pi W\phi_2}{e^2 s} = \left(\frac{M}{E} - \frac{\mu p M}{EW}\right)(1-\cos\theta) + (\mu^2-1)\left(\frac{M}{W} - \frac{E}{M}\right) \qquad (4.3)$$

$$\frac{8\pi W\phi_4}{e^2 s} = \left(-\frac{M}{E}\right)(1-\cos\theta) + (\mu^2+1)\frac{M}{W} - (\mu^2-1)\frac{W}{M} + \frac{2\mu^2 p}{E}$$

$$\frac{8\pi W\phi_6}{e^2 s} = \left(\frac{M}{E} + \frac{\mu p M}{EW}\right)(1-\cos\theta) + (\mu^2-1)\left(\frac{M}{W} - \frac{E}{M}\right)$$

$$\mu = \mu' + 1 \qquad s = \sin\frac{\theta}{2} \quad c = \cos\frac{\theta}{2}$$

Now, Gell-Mann and Goldberger[7] have shown that in the limit of small p the Compton amplitude must reduce to the classical result up to terms linear in p. This result, up to terms linear in p is given by

$$F = \frac{F_1^2}{M}\varepsilon_1\cdot\varepsilon_2 - 2\left(\frac{F_1}{2M} + F_2\right)^2 p\, i\sigma\cdot\left[(\hat{p}\times\varepsilon_2)\times(\hat{p}\times\varepsilon_1)\right]$$
$$- \frac{F_1}{2M}\left(\frac{F_1}{2M} + F_2\right)\mu p\left[\sigma\cdot\hat{p}(\hat{p}\times\varepsilon_1)\cdot\varepsilon_2 + \sigma\cdot\hat{p}\times\varepsilon_1\,\hat{p}\cdot\varepsilon_2\right.$$
$$\left. - \sigma\cdot\hat{p}'(\hat{p}'\times\varepsilon_2)\cdot\varepsilon_1 + \sigma\cdot\hat{p}'\times\varepsilon_2\,\hat{p}'\cdot\varepsilon_1\right] - \frac{F_1 F_2}{M} p\, i\sigma\cdot\varepsilon_1\times\varepsilon_2 \qquad (4.4)$$

We can check our result by finding its low energy limit and comparing it with (4.4). The low energy limit of (4.3) is given by

$$\frac{8\pi W\phi_1}{e^2 c} \longrightarrow -1 - \cos\theta + \frac{p}{M}\mu(1-\cos\theta)$$

$$
\begin{aligned}
\frac{8\pi W \phi_3}{e^2 c} &\longrightarrow -1 + \cos\theta + \frac{p}{M}(1-\mu^2) \\
\frac{8\pi W \phi_5}{e^2 c} &\longrightarrow -1 - \cos\theta - \frac{p}{M}\mu(1-\cos\theta) \\
\frac{8\pi W \phi_2}{e^2 s} &\longrightarrow +1 - \cos\theta + \frac{p}{M}\left[1-\mu^2-\mu(1-\cos\theta)\right] \\
\frac{8\pi W \phi_4}{e^2 s} &\longrightarrow +1 + \cos\theta \\
\frac{8\pi W \phi_6}{e^2 s} &\longrightarrow +1 - \cos\theta - \frac{p}{M}\left[1-\mu^2-\mu(1-\cos\theta)\right]
\end{aligned}
\tag{4.5}
$$

If one evaluates (4.4) between our helicity states one finds that the zero order term agrees but that it is necessary to add to (4.4) an additional term F'

$$
F' = \frac{e^2}{M}\frac{p}{M}(\hat{p}\cdot\varepsilon_2)(\hat{p}'\cdot\varepsilon_1) \tag{4.6}
$$

This term arises from the fact that the low energy limit derived by Gell-Mann and Goldberger is in the laboratory system while our result is in the center of mass. The additional term (4.6) comes in when we transform (4.3) into the center of mass and is required in order to insure that the photon polarization four-vector keeps its time component equal to zero. With this in mind we obtain for the low energy limit

$$
\frac{8\pi W \phi_1}{e^2 c} \longrightarrow -1 - \cos\theta + \frac{p}{M}\mu(1-\cos\theta)
$$

$$\frac{8\pi W \phi_3}{e^2 \mathcal{L}} \longrightarrow -1 + \cos\theta + \frac{p}{M}(1-\mu^2)$$

$$\frac{8\pi W \phi_5}{e^2 \mathcal{L}} \longrightarrow -1 - \cos\theta - \frac{p}{M}\mu(1-\cos\theta)$$

$$\frac{8\pi W \phi_2}{e^2 S} \longrightarrow +1 - \cos\theta + \frac{p}{M}\left[1-\mu^2-\mu(1-\cos\theta)\right]$$

$$\frac{8\pi W \phi_4}{e^2 S} \longrightarrow +1 + \cos\theta \qquad (4.7)$$

$$\frac{8\pi W \phi_6}{e^2 S} \longrightarrow +1 - \cos\theta - \frac{p}{M}\left[1-\mu^2-\mu(1-\cos\theta)\right]$$

which agrees with (4.5).

If we evaluate the Born term at 90° we obtain the result given in Table IV. To see to what extent the Born term contributes to the cross-section, apart from interference effects, we have plotted in Graph 2 the cross-section due to it alone. This is the Powell cross-section and its increasing with energy is due to the proton anomalous magnetic moment as can be seen by comparison with the Klein-Nishina cross-section which is obtained from (4.3) by setting $\mu = 1$ and is also plotted on Graph 2. Both agree at $p = 0$ (being equal to $\frac{1}{2}\left(\frac{e^2}{4\pi M}\right)^2$) which is expected since the effect of magnetic moment interactions go like v/c.

V. LOW AMPLITUDES

The importance of t-channel (Channel III) processes in Compton scattering was first noted by Low[23]. The diagrams of this type which we will consider are depicted in Figures 2e and 2f, corresponding to the exchange of a π^0 and an η meson. Since both these particles are pseudoscalars, the only difference being the π^0 is isovector and the η is isoscalar, the analysis of the two diagrams is the same.

For the π^0 we have at the π^0NN vertex

$$\langle \pi(q) | R | N_1 \bar{N}_2 \rangle = \frac{-iMg}{2\pi^{1/2}(p_{10}p_{20}q_0)^{1/2}} \bar{v}(p_2)\gamma_5 u(p_1) \qquad (5.1)$$

where g is the strong coupling constant $\left(\frac{g^2}{4\pi} = 15\right)$ and q is the momentum four-vector of the intermediate state. The γ_5 in the coupling is due to the fact that π^0 is a pseudoscalar particle.

At the $\pi^0\gamma\gamma$ vertex we have

$$\langle \gamma_1\gamma_2 | R^\dagger | \pi(q) \rangle = \frac{F(t)}{8\pi^{1/2}(k_{10}k_{20}q_0)^{1/2}} \varepsilon^+_{1\nu}\varepsilon^+_{2\mu} \times \varepsilon_{\mu\nu\rho\sigma}(k_1+k_2)_\rho (k_1-k_2)_\sigma \qquad (5.2)$$

where F(t) is the Goldberger-Treiman[24] form factor which at the mass of the pion assumes the value

$$F(m_\pi^2) \equiv F = -8\left(\frac{\pi}{m_\pi^3 \tau}\right)^{1/2} \qquad (5.3)$$

where τ is the pion decay lifetime.

Calculating the diagram, using these vertex functions we obtain for each of the six helicity amplitudes,

$$\phi_1 = \phi_3 = \phi_4 = \phi_5 = 0$$

$$\phi_2 = -\phi_6 = \frac{2p \sin\frac{\theta}{2}}{8\pi W} \quad \frac{\lambda}{t - m_\pi^2} \tag{5.4}$$

where $t = -\frac{(W^2 - M^2)^2}{2W^2}(1 - \cos\theta)$ and

$$\lambda = -4g(\pi m_\pi/\tau)^{1/2} = -2.1 \text{ MeV}$$

taking for the pion lifetime the current value of 1.9×10^{-16} sec[25]. The contribution of this diagram to the amplitude is given in Table V at 90° as a function of energy. Although it is comparitively small, the π^0 is important through interference with the other terms.

There has been some controversy in recent literature as to the sign of F. It is clear that all that matters is the sign of F relative to g which is arbitrarily made to be positive. Goldberger and Treiman's result is that Fg is negative, which was obtained by using dispersion relations at the $\pi^0\gamma\gamma$ vertex. A perturbation theory calculation, used by Jacob and Mathews[3] in their calculation of the contribution of the Low amplitude to Compton scattering at low energies has the opposite sign. Jacob and Mathews were able to obtain agreement with experiment at low energies with their choice of

sign, while Lapidus and Chou Kuang Chao[26] found that using the sign predicted by Goldberger and Treiman made the agreement with experiment worse. Several authors since then have avoided the issue by using both signs[4,27] while others have chosen either one or the other[8,9]. In any case, both calculations take into account only $N\bar{N}$ intermediate states and it is possible that other baryon-antibaryon intermediate states may be important. Furthermore, the prediction of the π^0 decay lifetime using Goldberger and Treiman's dispersion relations gives a result very different from that observed experimentally. For these reasons and for the reason that we can get good agreement in Compton scattering at low energies, we shall use the sign of Jacob and Mathews. In any case, at the energies being considered here and with the experimental uncertainties being what they are, this term will not play a very big role.

The contribution from the η-exchange diagram is calculated in exactly the same way. However, here we are on uncertain grounds as we know very little about the strength of the $\eta N\bar{N}$ coupling or the decay lifetime of the η. It is possible however, to make a theoretical estimate of these quantities by appealing to the results of unitary symmetry and the eight-fold way. The coupling $g_{\eta N\bar{N}}$ is given by $g_F\sqrt{3} - g_D/\sqrt{3}$ and if we use a D/F ratio of 3/2 predicted by SU(6) and verified approximately by the neutron and proton magnetic moments we find $g_{\eta N\bar{N}} = \frac{1}{5}\sqrt{3}\, g$. At the $\eta\gamma\gamma$ vertex we have conservation of U-spin, so that only the U = 0 state of the π^0 and η

can decay into two photons. Therefore the matrix element $\langle \frac{1}{2}\,\pi^0 + \frac{1}{2}\sqrt{3}\,\eta | 2\gamma \rangle = 0$, implying that $\langle \eta | 2\gamma \rangle = -\,1/\sqrt{3}\ \langle \pi^0 | 2\gamma \rangle$. Combining factors we get for λ in this case a value $(1/5\sqrt{3})(-1/\sqrt{3}) = -\,\frac{1}{5}$ that for π^0 exchange. In addition, the mass of the η now appears in the denominator so that the η-exchange contribution is much smaller than the π^0-exchange and will be neglected.

VI. CALCULATION OF CROSS-SECTIONS AND COMPARISON WITH EXPERIMENT

Using the amplitudes we have calculated and tabulated in Tables II, III, IV, and V, we proceed to add them together to obtain Table VII, the total amplitude. In order to show the effect of the Low amplitude, in Table VI is found the contribution due to the Born term and the isobar terms only. Using the expressions for the cross-sections obtained in Chapter II we calculate and plot the following quantities: (all at 90° CM)

Graph 1 $\left.\frac{d\sigma}{d\Omega}\right|_{\text{unpolarized}}$

Graph 2 a) $\left.\frac{d\sigma}{d\Omega}\right|_{\text{unpolarized}}$

b) $\left.\frac{d\sigma}{d\Omega}\right|_{\text{unpolarized}}$ with and without the Low amplitude

c) $\left.\frac{d\sigma}{d\Omega}\right|_{\text{unpolarized}}$ for the Born term alone (Powell amplitude)

d) $\left.\frac{d\sigma}{d\Omega}\right|_{\text{unpolarized}}$ for the Born term with $\mu = 1$ (Klein-Nishina amplitude)

Graph 3 $$\frac{\frac{d\sigma_{\perp}}{d\Omega} - \frac{d\sigma_{\parallel}}{d\Omega}}{\left.\frac{d\sigma}{d\Omega}\right|_{\text{unpolarized}}}$$

Graph 4 P, the recoil nucleon polarization.

The experimental data as of January 1966 consist of the following groups:

1) 0-100 MeV — Work done prior to 1960 and not applicable to this thesis.

2) 100 - 290 MeV — Illinois group of Bernardini et al.[29] at CM scattering angles of 90^{o} and 135^{o}.

3) 275 - 425 MeV — Cornell group of Dewire et al.[30] at 90^{o}. Also angular distribution at 312 MeV for 60^{o}, 75^{o}, 90^{o}, 120^{o}.

4) 300 - 700 MeV — Nagashima[31] at 90^{o}.

5) 500 - 850 MeV — M.I.T. group of Stiening et al.[11] at 90^{o}.

6) 450 - 1350 MeV — Cornell group of Rust et al.[12] at 90^{o} (most recent results).

The paucity of experiments on Compton scattering above the pion threshold is due to the great difficulty in performing them. Above the threshold the photoproduction of neutral pions produces photons via the process

$$p + \gamma \longrightarrow p + \pi^{o} \longrightarrow p + 2\gamma$$

with a cross-section about a hundred times greater than the Compton process itself. It is necessary to discriminate between these different events and this is done by measuring the nucleon recoil energy which is less for the photoproduction recoil protons than for the Compton recoil protons. This lowers the experimental efficiency

considerably so that most of the experiments have been done at 90^{o} in the CM which is an angle which tends to minimize the difficulty. So far, no experiments have been performed using polarized photons nor has the recoil nucleon polarization been measured.

On Graph 1 we have plotted the 90^{o} results of these experiments for comparison with the theoretical prediction of this thesis. In the region we are concerned with here the experimental errors are large so that we can only hope to make a general comparison and do not attempt to obtain fits nearly so accurate as those obtained with dispersion relations in the lower energy region.

VII. DISCUSSION

Using an isobar model we have obtained a theoretical Compton scattering cross-section curve which fits the main features of the experimental evidence. This agreement is sensitive to the accuracy of the model in the following ways:

1) There is good agreement with the value at the maximum of the first resonance. This depends very much on the accuracy of the value for C_3 and C_5 which we are using, as the cross-sections depend on the fourth power of these parameters. There is also a considerable contribution from the Born term which raises the peak by about 2.5×10^{-32} cm^2 over that due to the resonance alone.

2) At the second resonance there is disagreement between the results of Reference (11) and those of References (12) and (31) and our result favors the latter.

3) The positions of the maxima are shifted to lower energy for both resonances. This comes from interference between the real part of the resonance and the real background but its magnitude depends upon the large imaginary amplitude coming from the resonance which dominates the behavior of the cross-section at the peak. For the first resonance this background is mostly the Born term because the second resonance is weaker and has little effect at the position of the first. For the second resonance the tail of the first resonance is still large so that the back g round consists of both the Born term and the first resonance. The direction of this shift depends on the relative signs of the real part of the background and the imaginary part of the resonance at

energies just above and below the mass of the isobar. (See Appendix IV). In both cases our model predicts a relative sign which is positive so that the maxima are shifted to lower energies, more so for the second resonance because there the background and the resonance contributions are comparable.

4) The model exhibits the characteristic shallowness of the trough between the resonances. This comes from constructive interference between the resonances and would not occur if the relative signs of the amplitudes for the two resonances were not as they are. Also the Born term we have used (Powell amplitude) becomes even more important, as Graph 2 indicates it contributes more than two-thirds of the cross-section at the minimum.

5) The uncertainties in our model are larger than the contribution from the Low amplitude for π^0 exchange so that this would not be a very good way to measure the π^0 lifetime. If the η term which we have neglected were to be appreciable, that is if its lifetime were much shorter than we have supposed, its effect would be to raise the cross-section at the second resonance, lower it in between the resonances and raise it below the first resonance. If the M.I.T. data[11] turn out to be correct, this may be the reason why our model does not agree with it, another reason of course, being that the parameters D_3, D_5 which we have used are too small.

We conclude now with some observations about the results we have obtained for the recoil nucleon polarization and the cross-section for polarized photons.

1. Referring to Graph 4 we see that the recoil nucleon has positive polarization (in the y-direction see Figure 1) over the entire energy range 300 - 800 MeV and has a peak at about 600 MeV, of about 25 percent. The recoil nucleon polarization will be large and positive at energies where the amplitudes ϕ_3^*, ϕ_4 have large imaginary parts and the amplitudes $\phi_2 + \phi_6$, $\phi_1 + \phi_5$ have large real parts of the same sign or vice-versa. This condition holds between the resonances and hence we have the peak there. Note that the dashed part of the curve is an extrapolation down to 0 where we know that P is 0 since the Born amplitudes are all real. It is possible that P becomes negative for a while but we have not made any calculations in the sub-resonance region.

2. The Low amplitudes do not enter into the polarization because for these amplitudes we always have $\phi_2 = -\phi_6$ and we only have terms $\phi_2 + \phi_6$. Thus, the effect of a larger Low amplitude than we have considered would not change the general features of the curves (such as their sign) but would only increase or decrease them depending on whether the Low term subtracts from or adds to the unpolarized cross-section.

3. $\dfrac{\frac{d\sigma_\perp}{d\Omega} - \frac{d\sigma_\parallel}{d\Omega}}{\left.\frac{d\sigma}{d\Omega}\right|_{unp.}}$ exhibits a negative peak at the position of the first resonance and a positive peak at the second. This general feature depends only on the parity of the resonance as this is what mostly determines the relative signs of the amplitudes at the

resonance. An inspection of Tables II and III at the resonant energies shows that the signs observed with the full amplitude are those we get considering the resonances alone so that in our model the interference terms are not enough to change these signs. This would incidently, afford a means of determining the parity at a resonance if it were not already known.

Compton scattering may also be analyzed in terms of the multipole amplitudes of Chew, Goldberger, Low and Nambu[32] and this leads to a simple prediction for the angular dependence of the cross-section at resonance which is different from the result of the isobar model. This analysis will be found in Appendix V.

APPENDIX I. TRANSFORMATIONS BETWEEN AMPLITUDES

For convenience in comparing these results with those of other authors who use amplitudes other than helicity amplitudes, we are including here some other sets of amplitudes and the transformations from the helicity amplitudes used here.

A. Jacob and Mathews[3] use Pauli spinors:

$$\begin{aligned}\langle \gamma_2 N_2 | R | \gamma_1 N_1 \rangle = {} & g_1\, \varepsilon_1\cdot\varepsilon_2 + g_2 (k_2\cdot\varepsilon_1)(k_1\cdot\varepsilon_2) \\ & + g_3\, i\sigma\cdot\varepsilon_1\times\varepsilon_2 + g_4\, \varepsilon_1\cdot\varepsilon_2\, i\sigma\cdot k_1\times k_2 \\ & + g_5\, i\sigma\cdot(\varepsilon_1\cdot k_2\, \varepsilon_2\times k_1 - \varepsilon_2\cdot k_1\, \varepsilon_1\times k_2) \\ & + g_6\, i\sigma\cdot(\varepsilon_1\cdot k_2\, \varepsilon_2\times k_2 - \varepsilon_2\cdot k_1\, \varepsilon_1\times k_1)\end{aligned} \tag{AI.1}$$

$$f_i = \frac{2kM}{e^2} g_i$$

The momenta are unit vectors.

B. Lapidus and Chou Kuang-Chao[26] use Pauli spinors:

$$\begin{aligned}\langle \gamma_2 N_2 | R | \gamma_1 N_1 \rangle = {} & R_1\, \varepsilon_2\cdot\varepsilon_1 + R_2\, s_2\cdot s_1 + i R_3 \sigma\cdot\varepsilon_2\times\varepsilon_1 \\ & + i R_4 \sigma\cdot s_2\times s_1 + i R_5 (\sigma\cdot k_1\, s_2\cdot\varepsilon_1 - \sigma\cdot k_2\, s_1\cdot\varepsilon_2) \\ & + i R_6 (\sigma\cdot k_2\, s_2\cdot\varepsilon_1 - \sigma\cdot k_1\, s_1\cdot\varepsilon_2)\end{aligned} \tag{AI.2}$$

$$s_1 = k_1\times\varepsilon_1 \qquad s_2 = k_2\times\varepsilon_2$$

The momenta are unit vectors.

C. Hearn and Leader[6] use Dirac spinors.

Defining

$$P_\mu = \tfrac{1}{2}(p_{1\mu} - p_{2\mu}) \qquad K_\mu = \tfrac{1}{2}(k_{1\mu} - k_{2\mu})$$

$$P'_\mu = P_\mu - \frac{P\cdot K}{K^2} K_\mu \qquad Q_\mu = k_{1\mu} + k_{2\mu}$$

$$N_\mu = \epsilon_{\mu\nu\rho\sigma} P'_\nu K_\rho Q_\sigma$$

They write the amplitude in terms of invariant amplitudes A_i:

$$\langle \gamma_2 N_2 | F | \gamma_1 N_1 \rangle = \varepsilon^*_{2\nu}\, \bar{u}_2(-p_2)\, F_{\mu\nu}\, u_1(p_1)\, \varepsilon_{1\mu}$$

$$\left(T = \frac{M}{4\pi W} F \right)$$

$$F_{\mu\nu} = A_1(s,t,u)\frac{P'_\mu P_\nu}{P'^2} + A_2\frac{N_\mu N_\nu}{N^2} + A_3\frac{(P'_\mu N_\nu - P'_\nu N_\mu)}{(P'^2 N^2)^{1/2}} i\gamma_5$$

$$+ A_4\frac{P'_\mu P'_\nu}{P'^2} i\gamma\cdot K + A_5\frac{N_\mu N_\nu}{N^2} i\gamma\cdot K + A_6\frac{(P'_\mu N_\nu + P'_\nu N_\mu)}{(P'^2 N^2)^{1/2}} i\gamma_5 i\gamma\cdot K \qquad \text{(AI.3)}$$

The A_i are expressed in terms of the ϕ_i as follows:

A_i \ ϕ_i	$\frac{2\pi\phi_1}{pc}$	$\frac{2\pi\phi_3}{pc}$	$\frac{2\pi\phi_5}{pc}$	$\frac{2\pi\phi_2}{ps}$	$\frac{2\pi\phi_4}{ps}$	$\frac{2\pi\phi_6}{ps}$
A_1	M	-2M	M	-W	2W	-W
A_2	-M	-2M	-M	-W	-2W	-W
A_3	0	0	0	W	0	-W
A_4	$\frac{E}{p}$	$-\frac{2E}{p}$	$\frac{E}{p}$	$-\frac{M}{p}$	$+\frac{2M}{p}$	$-\frac{M}{p}$
A_5	$-\frac{E}{p}$	$-\frac{2E}{p}$	$-\frac{E}{p}$	$-\frac{M}{p}$	$-\frac{2M}{p}$	$-\frac{M}{p}$
A_6	- 1	0	1	0	0	0

(AI.4)

The f_i are expressed in terms of the ϕ_i as follows

f_i \ ϕ_i	ϕ_1/cp	ϕ_3/cp	ϕ_5/cp	ϕ_2/sp	ϕ_4/sp	ϕ_6/sp
f_1	$(1+\cos\theta)/4$	$(1+\cos\theta)/2$	$(1+\cos\theta)/4$	$-(1-\cos\theta)/4$	$-(1-\cos\theta)/2$	$-(1-\cos\theta)/4$
f_2	$-1/4$	$\frac{1+\cos\theta}{2(1-\cos\theta)}$	$-1/4$	$-1/4$	$\frac{1-\cos\theta}{2(1+\cos\theta)}$	$-1/4$
f_3	$-(1+\cos\theta)/4$	$-(1+\cos\theta)/2$	$(3-\cos\theta)/4$	$(1-\cos\theta)/4$	$(1-\cos\theta)/2$	$-(3+\cos\theta)/4$
f_4	$-1/4$	$-1/2$	$-1/4$	$-1/4$	$-1/2$	$-1/4$
f_5	$-1/4$	$\frac{\cos\theta}{2(1-\cos\theta)}$	$\frac{1-\cos\theta}{4(1+\cos\theta)}$	$-1/4$	$\frac{-\cos\theta}{2(1+\cos\theta)}$	$\frac{1+\cos\theta}{4(1-\cos\theta)}$
f_6	0	$\frac{-1}{2(1-\cos\theta)}$	$\frac{1}{2(1+\cos\theta)}$	0	$\frac{-1}{2(1+\cos\theta)}$	$\frac{-1}{2(1-\cos\theta)}$

(AI.5)

The f_i are expressed in terms of the R_i as follows:

$$
\begin{aligned}
f_1 &= - R_1 - R_2 \cos\theta \\
f_2 &= R_2 \\
f_3 &= R_3 + R_4 \cos\theta + (R_5 + R_6)(1 + \cos\theta) - (R_5 - R_6)(1 - \cos\theta) \\
f_4 &= R_4 \\
f_5 &= R_4 + R_5 \\
f_6 &= R_6 .
\end{aligned}
\qquad \text{(AI.6)}
$$

APPENDIX II. SPIN 5/2 PROPAGATOR

$$P_{\alpha_1\alpha_2\beta_1\beta_2} = \frac{1}{10M^2} \frac{M - i\not{p}}{M^2 + p^2} \times$$

$$5M^2 (\delta_{\alpha_1\beta_1} \delta_{\alpha_2\beta_2} + \delta_{\alpha_2\beta_1} \delta_{\alpha_1\beta_2} - \frac{2}{5} \delta_{\alpha_1\alpha_2} \delta_{\beta_1\beta_2})$$

$$+ \frac{4}{M^2} (p_{\alpha_1} p_{\alpha_2} p_{\beta_1} p_{\beta_2})$$

$$+ 2(\delta_{\alpha_1\alpha_2} p_{\beta_1} p_{\beta_2} + \delta_{\beta_1\beta_2} p_{\alpha_1} p_{\alpha_2} - 2\,\delta_{\alpha_1\beta_1} p_{\alpha_2} p_{\beta_2} - 2\delta_{\alpha_2\beta_1} p_{\alpha_1} p_{\beta_2} -$$

$$- 2\,\delta_{\alpha_1\beta_2} p_{\alpha_2} p_{\beta_1} - 2\delta_{\alpha_2\beta_2} p_{\alpha_1} p_{\beta_1})$$

$$+ M \left[\delta_{\alpha_1\beta_1} (\gamma_{\alpha_2} p_{\beta_2} - p_{\alpha_2} \gamma_{\beta_2}) + \delta_{\alpha_2\beta_1} (\gamma_{\alpha_1} p_{\beta_2} - p_{\alpha_1} \gamma_{\beta_2})\right.$$

$$\left. + \delta_{\alpha_1\beta_2} (\gamma_{\alpha_2} p_{\beta_1} - p_{\alpha_2} \gamma_{\beta_1}) + \delta_{\alpha_2\beta_2} (\gamma_{\alpha_1} p_{\beta_1} - p_{\alpha_1} \gamma_{\beta_1})\right]$$

$$+ \frac{2}{M} \left[- p_{\alpha_1} p_{\beta_1} (\gamma_{\alpha_2} p_{\beta_2} - p_{\alpha_2} \gamma_{\beta_2}) - p_{\alpha_2} p_{\beta_2} (\gamma_{\alpha_1} p_{\beta_1} - p_{\alpha_1} \gamma_{\beta_1})\right]$$

$$+ \left[\gamma_{\alpha_2} \gamma_{\beta_2} (p_{\alpha_1} p_{\beta_1} - M^2 \delta_{\alpha_1\beta_1}) + \gamma_{\alpha_1} \gamma_{\beta_2} (p_{\alpha_2} p_{\beta_1} - M^2 \delta_{\alpha_2\beta_1})\right.$$

$$\left. + \gamma_{\alpha_2} \gamma_{\beta_1} (p_{\alpha_1} p_{\beta_2} - M^2 \delta_{\alpha_1\beta_2}) + \gamma_{\alpha_1} \gamma_{\beta_1} (p_{\alpha_2} p_{\beta_2} - M^2 \delta_{\alpha_2\beta_2})\right] .$$

APPENDIX III. TABLE OF MATRIX ELEMENTS BETWEEN HELICITY STATES

Λ	$\langle + \vert \Lambda \vert + \rangle$	$\langle - \vert \Lambda \vert + \rangle$	$\langle + \vert \Lambda \vert - \rangle$	$\langle - \vert \Lambda \vert - \rangle$
1	c	$-\frac{E}{m}s$	$\frac{E}{m}s$	c
β	$\frac{E}{m}c$	$-s$	s	$\frac{E}{m}c$
$i\sqrt{2}\,\epsilon^{\alpha}$	$\frac{p}{m}s\,(1+\alpha)$	0	0	$-\frac{p}{m}s(1-\alpha)$
$i\sqrt{2}\,\beta\,\epsilon^{\alpha}$	0	$\frac{p}{m}c(1+\alpha)$	$\frac{p}{m}c(1-\alpha)$	0
$i\sqrt{2}\,\epsilon^{\alpha'}$	$-\frac{p}{m}s(1+\alpha')$	0	0	$\frac{p}{m}s(1-\alpha')$
$i\sqrt{2}\,\epsilon^{\alpha'}\beta$	0	$\frac{p}{m}c(1-\alpha')$	$\frac{p}{m}c(1+\alpha')$	0
$2\,\epsilon^{\alpha'}\epsilon^{\alpha}$	$c(1+\alpha)(1+\alpha')$	$-\frac{E}{m}s(1-\alpha')(1+\alpha)$	$\frac{E}{m}s(1+\alpha')(1-\alpha)$	$c(1-\alpha')(1-\alpha)$
$2\beta\,\epsilon^{\alpha'}\epsilon^{\alpha}$	$\frac{E}{m}c(1+\alpha')(1+\alpha)$	$-s(1-\alpha')(1+\alpha)$	$s(1+\alpha')(1-\alpha)$	$\frac{E}{m}c(1-\alpha')(1-\alpha)$

APPENDIX IV. SHIFTING OF RESONANT PEAKS

In general, near a resonance, the background is real and slowly varying so we may write for some amplitude

$$f(E) = B + \frac{\alpha + i\beta}{\alpha^2 + \beta^2}$$

For the cross-section we will have terms

$$\sigma(E) \sim |f(E)|^2 = B^2 + \frac{1}{\alpha^2 + \beta^2} + \frac{2\alpha B}{\alpha^2 + \beta^2}$$

To find the maximum we set $\sigma'(E) = 0$ using the fact that in the neighborhood of the maximum $\alpha \ll \beta$ and we can also neglect the derivative of B. Then we have

$$\sigma'(E) \approx -\frac{2\alpha}{\beta^4} + \frac{2B}{\beta^2} = 0$$

so the maximum occurs when $\alpha = \beta^2 B$ or in the direction from the original peak where B and α have the same sign.

For the first resonance in Compton scattering we see that for all the amplitudes except ϕ_3 we get a positive sign at lower energies so the peak shifts to the left. Similarly at the second resonance we find that ϕ_1, ϕ_3, ϕ_4, ϕ_6 give positive contributions and ϕ_3, ϕ_4 negative, but with a resultant shift to the left.

APPENDIX V. MULTIPOLE ANALYSIS

In this section we shall decompose the Compton helicity amplitude into partial waves and relate the imaginary part of these to photoproduction partial wave helicity amplitudes via unitarity. We shall compare this at the first resonance where the amplitude is predominantly imaginary, with the result of the isobar model.

The six helicity amplitudes ϕ_i can be decomposed into partial waves

$$\phi_i = \phi_{\lambda_1,\lambda_2} = \frac{1}{2p} \sum_J (2J+1)\, \phi^J_{\lambda_1,\lambda_2}\, d^J_{\lambda_1,\lambda_2}(\theta) \qquad \text{(AV.1)}$$

where $\lambda_1 = \lambda N_1 - \lambda\gamma_1$, $\lambda_2 = \lambda N_2 - \lambda\gamma_2$, the $\phi^J_{\lambda_1\lambda_2}$ are the partial wave helicity amplitudes describing a transition from a state of helicity λ_1 and total angular momentum J to a state of helicity λ_2 and total angular momentum J, and $d^J_{\lambda_1\lambda_2}(\theta)$ are the well-known functions given by Jacob and Wick[16].

Now, since the S matrix is unitary

$$S^+S = I \qquad \text{(AV.2)}$$

we can relate the imaginary part of the Compton scattering amplitude to the pion photoproduction amplitudes. These four amplitudes can also be expanded into partial waves,

$$\varphi_i = \varphi_{\lambda_1,\lambda_2} = \frac{1}{2(pq)^{1/2}} \sum_J (2J+1)\, \varphi^J_{\lambda_1,\lambda_2}\, d^J_{\lambda_1,\lambda_2}(\theta) \qquad \text{(AV.3)}$$

where q is the pion momentum. From AV.1, AV.2, & AV.3 it follows that

$$Im\,\phi^{J}_{\lambda_1,\lambda_2} = \frac{1}{2}\sum_{\lambda=\pm\frac{1}{2}} \varphi^{J}_{\lambda_1,\lambda}\,\varphi^{J\,*}_{\lambda\lambda_2} \qquad \text{(AV.4)}$$

We now make the usual assumption that at the position of the resonances only the partial waves with J = 3/2 occur in AV.4 so that

$$Im\,\phi_{\lambda_1,\lambda_2} = \frac{1}{p}\left(\varphi^{3/2}_{\lambda_1,\frac{1}{2}}\,\varphi^{3/2\,*}_{\lambda_2,\frac{1}{2}} + \varphi^{3/2}_{\lambda_1,-\frac{1}{2}}\,\varphi^{3/2\,*}_{\lambda_2,-\frac{1}{2}}\right) d^{3/2}_{\lambda_1,\lambda_2}(\theta) \qquad \text{(AV.5)}$$

Now we shall turn to the expression of the photoproduction partial wave helicity amplitudes in terms of the electric and magnetic multipole amplitudes of Chew, Goldberger, Low and Nambu[32], obtained by evaluating equation (7.2) of Reference (32) between photoproduction helicity states and using (7.3) - (7.6) of (32). The result is

$$\begin{aligned}
\varphi^{3/2}_{-\frac{1}{2}\,\frac{1}{2}} &= \left(\frac{pq}{2}\right)^{1/2}\left[M_{1+} + 3E_{1+} + 3M_{2-} - E_{2-}\right] \\
\varphi^{3/2}_{\frac{1}{2}\,\frac{1}{2}} &= \left(\frac{pq}{2}\right)^{1/2}\left[M_{1+} + 3E_{1+} - 3M_{2-} + E_{2-}\right] \\
\varphi^{3/2}_{-\frac{3}{2}\,\frac{1}{2}} &= \left(\frac{pq}{2}\right)^{1/2}\sqrt{3}\left[M_{1+} - E_{1+} - M_{2-} - E_{2-}\right] \\
\varphi^{3/2}_{-\frac{3}{2}\,-\frac{1}{2}} &= \left(\frac{pq}{2}\right)^{1/2}\sqrt{3}\left[-M_{1+} + E_{1+} - M_{2-} - E_{2-}\right]
\end{aligned} \qquad \text{(AV.6)}$$

Now the first resonance proceeds mostly via M_{1+} with a small amount of E_{1+} and likewise the second resonance proceeds via E_{2-} and M_{2-}. Therefore, at the first resonance we have

$$
\begin{aligned}
Im\,\phi_1 &= 2\,|M_{1+} + 3E_{1+}|^2 \; d^{3/2}_{-\frac{1}{2}-\frac{1}{2}}(\theta) \\
Im\,\phi_2 &= 2\,|M_{1+} + 3E_{1+}|^2 \; d^{3/2}_{-\frac{1}{2}\frac{1}{2}}(\theta) \\
Im\,\phi_3 &= 2\sqrt{3}\,|(M_{1+}+3E_{1+})(M_{1+}-E_{1+})^*| \; d^{3/2}_{-\frac{1}{2}\frac{3}{2}}(\theta) \\
Im\,\phi_4 &= 2\sqrt{3}\,|(M_{1+}+3E_{1+})(M_{1+}-E_{1+})^*| \; d^{3/2}_{-\frac{1}{2}-\frac{3}{2}}(\theta) \\
Im\,\phi_5 &= 6\,|M_{1+}-E_{1+}|^2 \; d^{3/2}_{-\frac{3}{2}-\frac{3}{2}}(\theta) \\
Im\,\phi_6 &= 6\,|M_{1+}-E_{1+}|^2 \; d^{3/2}_{\frac{3}{2}-\frac{3}{2}}(\theta)
\end{aligned}
\qquad \text{(AV.7)}
$$

where a constant in front has been omitted as we are interested in the angular dependence. If we assume pure magnetic dipole by setting $E_{1+} = 0$, and substitute the values for the d-functions we obtain

$$
\begin{aligned}
&Im\,\phi_1 = |M_{1+}|^2(1-3\cos\theta)\cos\tfrac{\theta}{2}\,; \quad Im\,\phi_5 = -|M_{1+}|^2 3(1+\cos\theta)\cos\tfrac{\theta}{2} \\
&Im\,\phi_2 = |M_{1+}|^2(1+3\cos\theta)\sin\tfrac{\theta}{2}\,; \quad Im\,\phi_6 = -|M_{1+}|^2 3(1-\cos\theta)\sin\tfrac{\theta}{2} \\
&Im\,\phi_3 = |M_{1+}|^2 3(1-\cos\theta)\cos\tfrac{\theta}{2} \qquad \text{(AV.8)} \\
&Im\,\phi_4 = -|M_{1+}|^2 3(1+\cos\theta)\sin\tfrac{\theta}{2}
\end{aligned}
$$

$$
\text{At } 90°: \; 3|\phi_1| = 3|\phi_2| = |\phi_3| = |\phi_4| = |\phi_5| = |\phi_6|
$$

Since at the resonance Re ϕ_i is almost zero we can use (AV.8) to calculate the cross-section at the resonance as a function of angle since the same factor $|M_{1+}|^2$ appears in each helicity amplitude. The result is

$$\left.\frac{d\sigma}{d\Omega}\right|_{M_R} \sim |M_{1+}|^2 \left(7 + 3\cos^2\theta\right) \qquad \text{(AV.9)}$$

At the second resonance we must retain E_{2-} and M_{2-}

$$\begin{aligned}
Im\,\phi_1 &= 2\,|3M_{2-} - E_{2-}|^2\, d^{3/2}_{-\frac{1}{2}-\frac{1}{2}}(\theta)\\
Im\,\phi_2 &= -2\,|3M_{2-} - E_{2-}|^2\, d^{3/2}_{-\frac{1}{2}\frac{1}{2}}(\theta)\\
Im\,\phi_3 &= -2\sqrt{3}\,|(3M_{2-} - E_{2-})(-M_{2-} - E_{2-})^*|\, d^{3/2}_{-\frac{1}{2}-\frac{3}{2}}(\theta)\\
Im\,\phi_4 &= 2\sqrt{3}\,|(3M_{2-} - E_{2-})(-M_{2-} - E_{2-})^*|\, d^{3/2}_{-\frac{1}{2}-\frac{3}{2}}(\theta) \qquad \text{(AV.10)}\\
Im\,\phi_5 &= 2\,|-M_{2-} - E_{2-}|^2\, d^{3/2}_{-\frac{3}{2}-\frac{3}{2}}(\theta)\\
Im\,\phi_6 &= -2\,|-M_{2-} - E_{2-}|^2\, d^{3/2}_{\frac{3}{2}-\frac{3}{2}}(\theta)
\end{aligned}$$

and with the assumption that E_{2-} dominates

$$\begin{aligned}
Im\,\phi_1 &= |E_{2-}|^2(1-3\cos\theta)\cos\tfrac{\theta}{2} \qquad Im\,\phi_5 = |E_{2-}|^2 3(-1-\cos\theta)\cos\tfrac{\theta}{2}\\
Im\,\phi_2 &= |E_{2-}|^2(-1-3\cos\theta)\sin\tfrac{\theta}{2} \qquad Im\,\phi_6 = |E_{2-}|^2 3(1-\cos\theta)\sin\tfrac{\theta}{2}\\
Im\,\phi_3 &= |E_{2-}|^2 3(-1-\cos\theta)\cos\tfrac{\theta}{2} \qquad \text{(AV.11)}\\
Im\,\phi_4 &= |E_{2-}|^2 3(1+\cos\theta)\sin\tfrac{\theta}{2}
\end{aligned}$$

$$\text{At } 90^\circ\text{: } 3|\phi_1| = 3|\phi_2| = |\phi_3| = |\phi_4| = |\phi_5| = |\phi_6|$$

so that the cross-section at the second resonance becomes

$$\left.\frac{d\sigma}{d\Omega}\right|_{M_R} \sim |E_{2-}|^2 (7 + 3\cos^2\theta) \qquad \text{(AV.12)}$$

which has the same angular dependence as the first resonance.

Let us compare this result now with that obtained for the angular distribution by the isobar model. Considering only the isobar terms we have, for the first resonance, setting $W = M_R$, $E = E_R$ and $k = k_R$, a great simplification of (3.25):

$$\Delta^2 \phi_1 \frac{8\pi}{e^2} = \left[a^2\left(-k_R^2 \frac{M}{M_R}\right) + b^2 k_R^2 M_R^2 \frac{E_R - M}{2M}\right] \frac{1}{3}(3\cos\theta - 1)\cos\frac{\theta}{2}$$

$$\Delta^2 \phi_3 \frac{8\pi}{e^2} = \left[a^2 k_R^2 + b^2 k_R^2 M_R^2 \frac{E_R - M}{2M} + ab k_R^3 \frac{E_R}{M}\right](1 - \cos\theta)\cos\frac{\theta}{2}$$

$$\Delta^2 \phi_5 \frac{8\pi}{e^2} = \left[a^2\left(-k_R^2 \frac{E_R}{M}\right) + b^2 k_R^2 M_R^2 \frac{E_R - M}{2M}\right](1 + \cos\theta)\cos\frac{\theta}{2}$$

$$\Delta^2 \phi_2 \frac{8\pi}{e^2} = \left[a^2 k_R^2 \frac{M}{M_R} - b^2 k_R^2 M_R^2 \frac{E_R - M}{2M}\right] \frac{1}{3}(3\cos\theta + 1)\sin\frac{\theta}{2} \qquad \text{(AV.13)}$$

$$\Delta^2 \phi_4 \frac{8\pi}{e^2} = \left[a^2 k_R^2 + b^2 k_R^2 M_R^2 \frac{E_R - M}{2M} + ab\, k_R^3 \frac{E_R}{M}\right](1 + \cos\theta)\sin\frac{\theta}{2}$$

$$\Delta^2 \phi_6 \frac{8\pi}{e^2} = \left[a^2\left(-k_R^2 \frac{M_R}{M}\right) + b^2 k_R^2 M_R^2 \frac{E_R - M}{2M}\right](1 - \cos\theta)\sin\frac{\theta}{2}$$

where we observe that each amplitude has the angular dependence of the appropriate d-function. Numerically, the terms with b are negligible compared to the a^2 term so we have

$$\begin{aligned} \phi_1 &\sim -\frac{k_R^2 M}{M_R}(3\cos\theta - 1)\cos\frac{\theta}{2} \\ \phi_3 &\sim k_R^2\, 3(1 - \cos\theta)\cos\frac{\theta}{2} \qquad \text{(AV.14} \\ \phi_5 &\sim \frac{-k_R^2 M_R}{M} 3(1 + \cos\theta)\cos\frac{\theta}{2} \end{aligned}$$

$$\phi_2 \sim \frac{k_R^2 M}{M_R}(3\cos\theta + 1)\sin\frac{\theta}{2}$$

$$\phi_4 \sim k_R^2\, 3(1+\cos\theta)\sin\frac{\theta}{2}$$

$$\phi_6 \sim \frac{-k_R^2 M_R}{M}\, 3(1-\cos\theta)\sin\frac{\theta}{2}$$

Comparison with (V.7) and (V.8) shows that instead of the single factor $|M_{1+}|^2$ as in (V.8) we have three different non-angular factors as in (V.7) with that for ϕ_1 equalling that for ϕ_2, $\phi_3 = \phi_4$ and $\phi_5 = \phi_6$. We can identify the three factors in (V.14) with those in (V.7)

$$|M_{1+} + 3E_{1+}|^2 \longrightarrow \frac{k_R^2 M}{M_R}$$

$$|M_{1+} - E_{1+}|^2 \longrightarrow \frac{k_R^2 M_R}{M} \qquad \text{(AV.15)}$$

$$|(M_{1+} + 3E_{1+})(M_{1+} - E_{1+})^*| \longrightarrow k_R^2$$

so that it becomes obvious how our analysis by isobars has included an electric quadrupole part. In fact, we can estimate immediately how much electric quadrupole is included by satisfying (AV.15) with

$$M_{1+} - E_{1+} = \frac{M_R}{M}(M_{1+} + 3E_{1+}) \qquad \text{(AV.16)}$$

so that

$$\rho = \left|\frac{E_{1+}}{M_{1+}}\right| = \left|\frac{M - M_R}{M + 3M_R}\right| \approx 6.5\% \qquad \text{(AV.17)}$$

If we substitute numerical values in (AV.13) we obtain for the cross-section at the first resonance as a function of angle due to

the N* alone

$$\left.\frac{d\sigma}{d\Omega}\right|_{M_R = M_{N^*}} \approx (11.5 + 9.9\cos^2\theta) \times 10^{-32}\ cm^2 \qquad \text{(AV.18)}$$

as compared with the angular dependence $7 + 3\cos^2\theta$ obtained from the multipole analysis, assuming pure magnetic dipole. These two angular dependencies have been plotted as Graph 5 where experimental points at the nearest available energy are shown. The magnetic dipole and isobar angular distributions have been normalized to give the 90° cross-section from experiment at M_R and the vertical numerical scale should not be taken seriously as for both these curves the non-resonant contributions have been neglected. What the graph does illustrate is that the isobar model reproduces the sharpness of the experimental angular distribution much better than the $7 + 3\cos^2\theta$ and a more careful angular distribution experiment would be able to decide the extent to which electric quadrupole is important.

In a similar manner we obtain from the N** isobar an angular distribution at 750 MeV,

$$\left.\frac{d\sigma}{d\Omega}\right|_{M_R = M_{N^{**}}} \approx 17 + 31\cos^2\theta \qquad \text{(AV.19)}$$

as compared with the $7 + 3\cos^2\theta$ assuming only E_{2-}. The big difference here comes from the large amount of M_{2-} we have included. There are no experimental points at angles other than 90° in this region.

TABLE I

HELICITY AMPLITUDES

λN_2	$\lambda\gamma_2$	λN_1	$\lambda\gamma_1$	λ_1	λ_2	Name
1/2	1	1/2	1	- 1/2	- 1/2	ϕ_1
- 1/2	1	1/2	1	- 1/2	- 3/2	ϕ_4
1/2	- 1	1/2	1	- 1/2	3/2	ϕ_3
- 1/2	- 1	1/2	1	- 1/2	1/2	ϕ_2
1/2	1	1/2	- 1	3/2	- 1/2	ϕ_3
- 1/2	1	1/2	- 1	3/2	- 3/2	ϕ_6
1/2	- 1	1/2	- 1	3/2	3/2	ϕ_5
- 1/2	- 1	1/2	- 1	3/2	1/2	ϕ_4
1/2	1	- 1/2	1	- 3/2	- 1/2	$-\phi_4$
- 1/2	1	- 1/2	1	- 3/2	- 3/2	ϕ_5
1/2	- 1	- 1/2	1	- 3/2	3/2	$-\phi_6$
- 1/2	- 1	- 1/2	1	- 3/2	1/2	ϕ_3
1/2	1	- 1/2	- 1	1/2	- 1/2	$-\phi_2$
- 1/2	1	- 1/2	- 1	1/2	- 3/2	ϕ_3
1/2	- 1	- 1/2	- 1	1/2	3/2	$-\phi_4$
- 1/2	- 1	- 1/2	- 1	1/2	1/2	ϕ_1

$\lambda_1 = \lambda N_1 - \lambda\gamma_1 \qquad \lambda_2 = \lambda N_2 - \lambda\gamma_2$

TABLE II

FIRST RESONANCE(90^{o})

W \ $8\pi W\phi_i / e^2\sqrt{\frac{1}{2}}$	1	3	5	2	4	6
1210	-.45 - i1.34	-1.28 - i4.00	1.85 + i5.36	-.36 - i1.03	-1.35 - i3.94	1.90 + i5.47
1220	-.28 - i1.41	-1.14 - i4.50	1.54 + i6.45	-.24 - i1.17	-1.12 - i4.41	1.54 + i6.55
1230	-.15 - i1.44	- .55 - i5.30	+.76 + i7.30	-.14 - i1.35	- .55 - i5.20	+.76 + i7.30
1240	0 - i1.45	0 - i5.41	0 + i7.55	0 - i1.45	0 - i5.41	0 + i7.55
1250	.22 - i1.45	.80 - i5.20	-0.9 + i7.7	.22 - i1.42	.80 - i5.2	-0.9 + i7.7
1260	.42 - i1.40	1.5 - i5.0	-2.1 + i7.8	.42 - i1.40	1.5 - i5.0	-2.1 + i7.8
1300	.69 - i1.00	2.4 - i3.6	-3.5 + i4.8	.70 - i1.05	2.5 - i3.7	-3.5 + i4.8
1400	.64 - i .32	2.0 - i1.0	-3.0 + i1.5	.68 - i .34	2.0 - i1.0	-3.0 + i1.5
1515	.42 - i .12	1.28 - i .35	-1.9 + i .50	.44 - i .14	1.28 - i .35	-1.9 + i .50

TABLE III

SECOND RESONANCE (90^{o})

W \ $8\pi W\phi_i/e^2\sqrt{\frac{1}{2}}$	1	3	5	2	4	6
1210	- .35 - i.10	+ .94 + i .20	.80 + i .17	.30 + i.09	- .94 - i .20	- .80 - i .17
1220	- .35 - i.12	.96 + i .25	.82 + i .23	.33 + i.11	- .96 - i .25	- .82 - i .23
1230	- .36 - i.12	.98 + i .30	.85 + i .25	.34 + i.11	- .99 - i .30	- .85 - i .25
1240	- .38 - i.13	+ 1.00 + i .32	.90 + i .28	.33 + i.12	- 1.00 - i .32	- .92 - i .29
1250	- .39 - i.14	1.04 + i .34	.95 + i .30	.34 + i .13	- 1.05 - i .33	- .97 - i .31
1260	- .40 - i.15	1.10 + i .40	1.0 + i .35	.35 + i .13	- 1.12 - i .37	- 1.2 - i .37
1300	- .45 - i.20	1.20 + i .49	1.1 + i .45	.38 + i .18	- 1.20 - i .50	- 1.3 - i .45
1400	- .68 - i.49	1.64 + i1.20	1.5 + i1.1	.67 + i .48	- 1.65 - i1.20	- 1.6 - i1.1
1515	0 - i1.2	0 + i3.44	0 + i3.24	0 + i1.16	0 - i3.44	0 - i3.24

TABLE IV

BORN TERM (90^{o})

W \ $8\pi\phi_i W/e^2\sqrt{\frac{1}{2}}$	1	3	5	2	4	6
940	- 1.00	- 1.00	- 1.00	+ 1.00	+ 1.00	+ 1.00
1210	- 1.05	+ 0.37	+ 0.33	- 2.61	- 1.88	+ 1.54
1220	- 1.05	+ 0.40	+ 0.36	- 2.70	- 1.95	+ 1.61
1230	- 1.06	+ 0.44	+ 0.39	- 2.81	- 2.05	+ 1.68
1240	- 1.07	+ 0.49	+ 0.44	- 2.90	- 2.11	+ 1.74
1250	- 1.07	+ 0.54	0.50	- 3.0	- 2.3	1.82
1260	- 1.03	+ 0.60	0.55	- 3.1	- 2.6	1.95
1300	- 1.00	+ 0.80	0.75	- 3.6	- 3.0	2.2
1400	- .97	+ 1.4	1.40	- 4.8	- 3.7	3.2
.515	- .47	+ 2.2	2.4	- 6.0	- 3.9	4.4

TABLE V

LOW AMPLITUDE (90^{o})

($\tau_{\pi^0} = 1.9 \times 10^{-16}$ sec)

W \ $8\pi W\phi_i / e^2\sqrt{\frac{I}{2}}$	2
940	0
1210	.73
1220	.72
1230	.72
1240	.71
1250	.68
1260	.67
1300	.61
1400	.51
1515	.43

$\phi_6 = -\phi_2$

$\phi_1 = \phi_3 = \phi_4 = \phi_5 = 0$

TABLE VI

ISOBARS + BORN TERM ($\tau_{\pi 0} = \infty$) (90^{o})

W \ $8\pi W\phi_i / e^2\sqrt{\frac{1}{2}}$	1	3	5	2	4	6
940	-1.0 + i0	-1.0 + i0	-1.0 + i0	1.0 + i0	1.0 + i0	1.0 + i0
1210	-1.80 - i1.44	-.08 - i3.80	2.98 + i5.53	-2.67 - i .94	-4.17 - i4.14	2.73 + i5.36
1220	-1.58 - i1.53	.22 - i4.25	2.72 + i6.68	-2.61 - i1.06	-4.03 - i4.66	2.33 + i6.32
1230	-1.58 - i1.56	.87 - i5.00	2.00 + i7.55	-2.61 - i1.24	-3.61 - i5.50	1.60 + i7.05
1240	-1.45 - i1.58	1.49 - i5.09	1.34 + i7.93	-2.56 - i1.33	-3.11 - i5.73	0.82 + i7.25
1250	-1.24 - i1.59	2.38 - i4.86	0.55 + i8.0	-2.44 - i1.29	-2.45 - i5.53	-.18 + i7.4
1260	-1.01 - i1.55	3.2 - i4.60	-0.55 + i8.2	-2.33 - i1.27	-2.20 - i5.37	-1.3 + i7.4
1300	- .76 - i1.20	4.4 - i3.1	-1.65 + i5.3	-2.5 - i0.87	-1.70 - i4.20	-2.4 + i4.3
1400	-1.01 - i .52	5.0 + i .20	-0.1 + i2.6	-3.5 + i0.14	-3.4 - i2.2	-1.4 + i0.40
1515	- .05 - i .61	3.48 + i3.09	0.5 + i3.74	-5.6 + i1.02	-2.6 - i3.09	2.5 - i2.74

TABLE VII

TOTAL AMPLITUDE (90^{o})

W \ $8\pi W\phi_i / e^2\sqrt{\frac{1}{2}}$	1	3	5	2	4	6
940	-1.00 + i0	-1.00 + i0	-1.00 + i0	+1.00 + i0	+1.00 + i0	+1.00 + i0
1210	-1.85 - i1.44	-.08 - i3.8	2.98 + i5.53	-1.94 - i0.94	-4.17 - i4.14	2.00 + i5.36
1220	-1.58 - i1.53	0.22 - i4.25	2.72 + i6.68	-1.89 - i1.06	-4.03 - i4.66	1.65 + i6.32
1230	-1.58 - i1.56	0.87 - i5.00	2.00 + i7.55	-1.89 - i1.24	-3.61 - i5.50	1.92 + i7.05
1240	-1.45 - i1.58	1.49 - i5.09	1.34 + i7.93	-1.85 - i1.33	-3.11 - i5.73	0.13 + i7.25
1250	-1.24 - i1.59	2.38 - i4.86	0.55 + i8.0	-1.76 - i1.29	-2.45 - i5.53	-0.90 + i7.4
1260	-1.01 - i1.55	3.20 - i4.60	-0.55 + i8.2	-1.66 - i1.27	-2.20 - i5.37	-2.00 + i7.4
1300	-0.76 - i1.20	4.4 - i3.1	-1.65 + i5.3	-1.89 - i0.87	-1.70 - i4.20	-3.0 + i4.3
1400	-1.01 - i .52	5.0 + i0.20	-0.1 + i2.6	-2.94 + i0.14	-3.4 - i2.2	-1.90 + i0.40
1515	- .05 - i .61	3.5 + i3.1	0.5 + i3.74	-5.2 + i1.02	-2.6 - i3.09	2.10 - i2.74

TABLE VIII

PROPERTIES OF ISOBARS

	N^*		N^{**}
$J^P T$	$\frac{3}{2}+, \frac{3}{2}$		$\frac{3}{2}-, \frac{1}{2}$
Mass	1240 MeV		1515 MeV
$k\gamma_{lab}$	360 MeV		750 MeV
Width	140 MeV		140 MeV
C_3	.35	D_3	-.048
C_5	-.0043	D_5	-.009
a^2	5.7×10^{-6} e^2 MeV^{-2}	c^2	$.11 \times 10^{-6}$ e^2 MeV^{-2}
b^2	1.65×10^{-13} e^2 MeV^{-4}	d^2	8.2×10^{-13} e^2 MeV^{-4}
ab	$-.97 \times 10^{-9}$ e^2 MeV^{-3}	Cd	$-.30 \times 10^{-9}$ e^2 MeV^{-3}

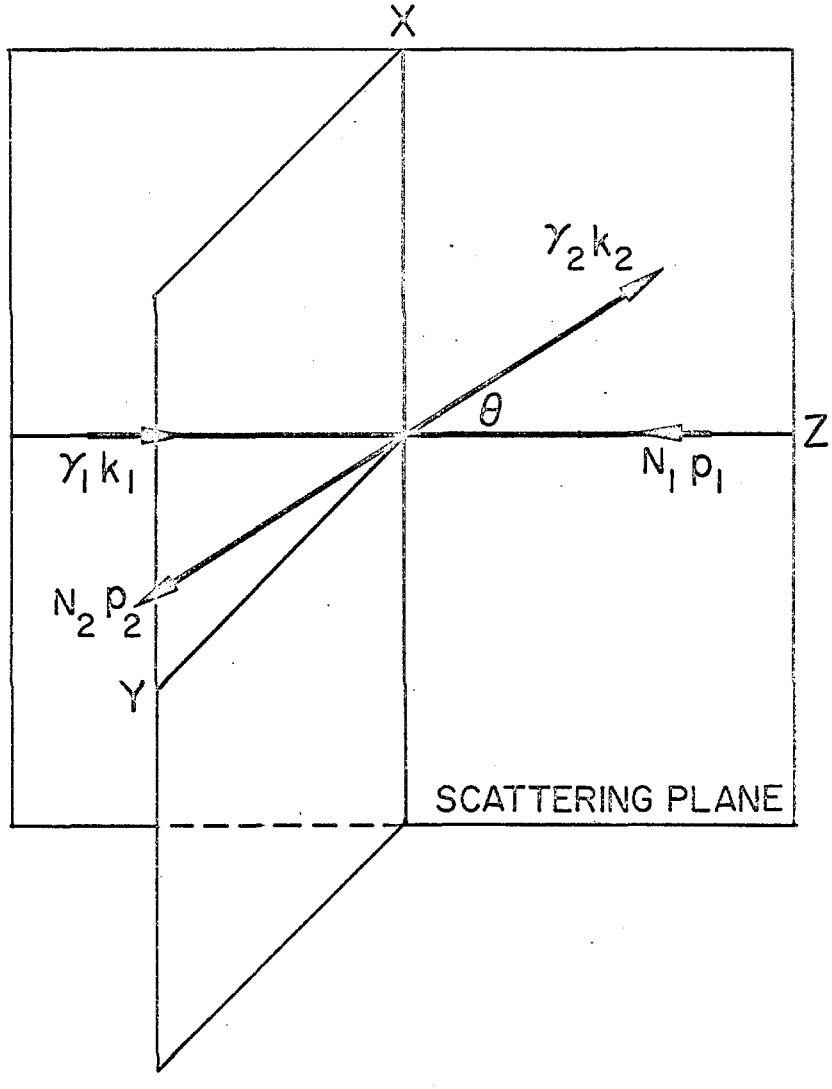

FIGURE 1

CENTER OF MASS COORDINATES

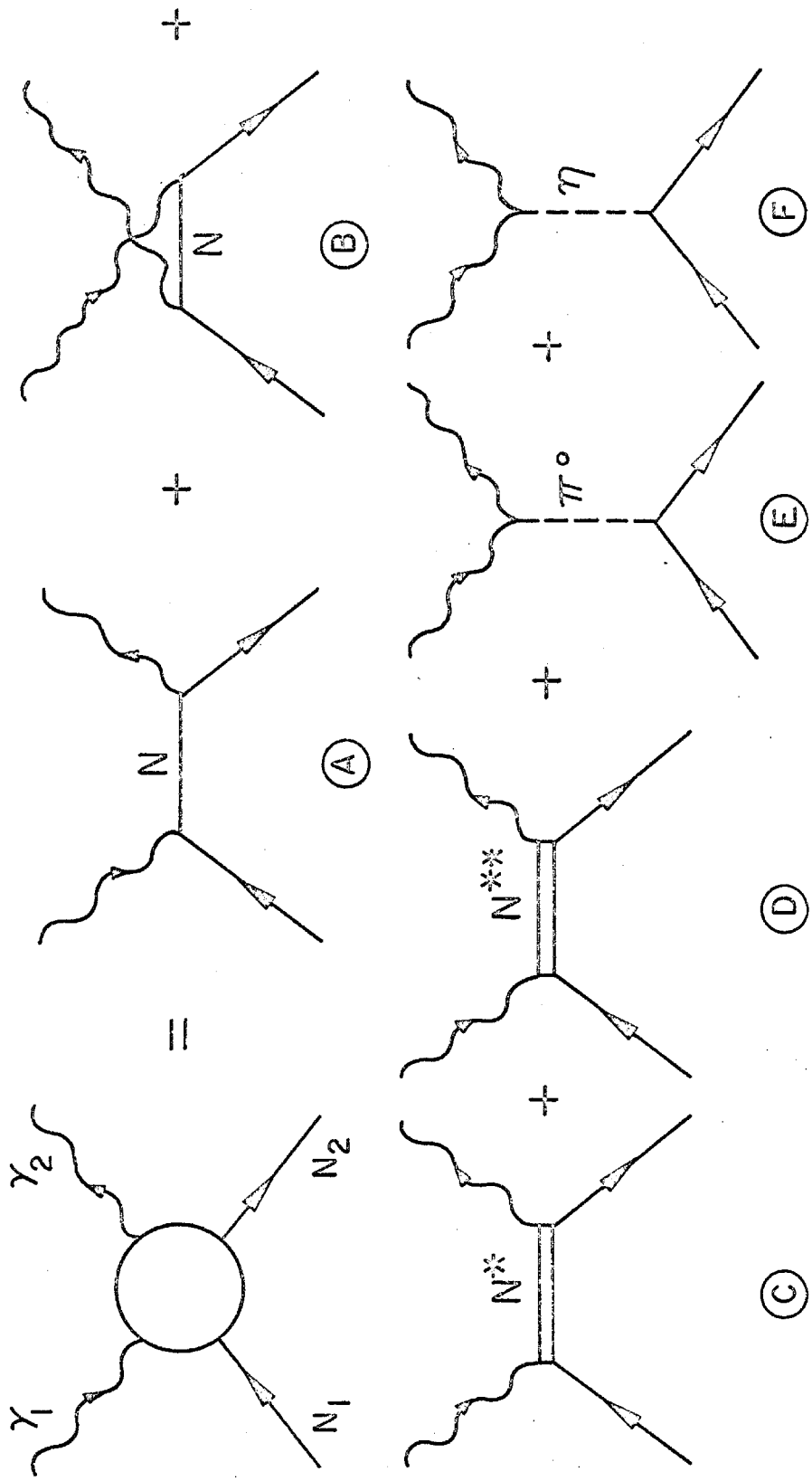

FIGURE 2

FEYNMAN GRAPHS USED

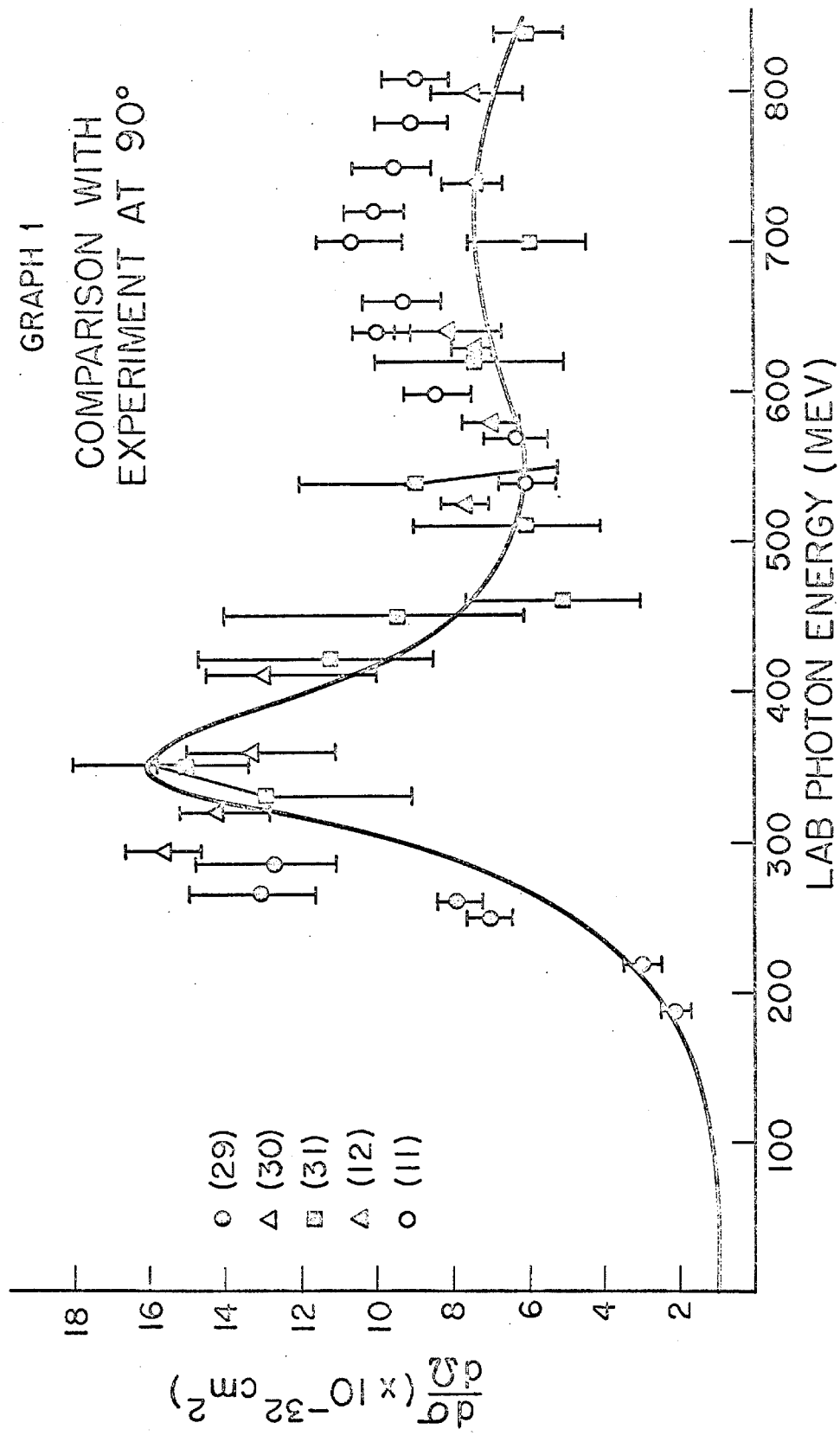
GRAPH 1
COMPARISON WITH
EXPERIMENT AT 90°
$\frac{d\sigma}{d\Omega}$ ($\times 10^{-32}$ cm^2)
LAB PHOTON ENERGY (MEV)
(29)
(30)
(31)
(12)
(11)

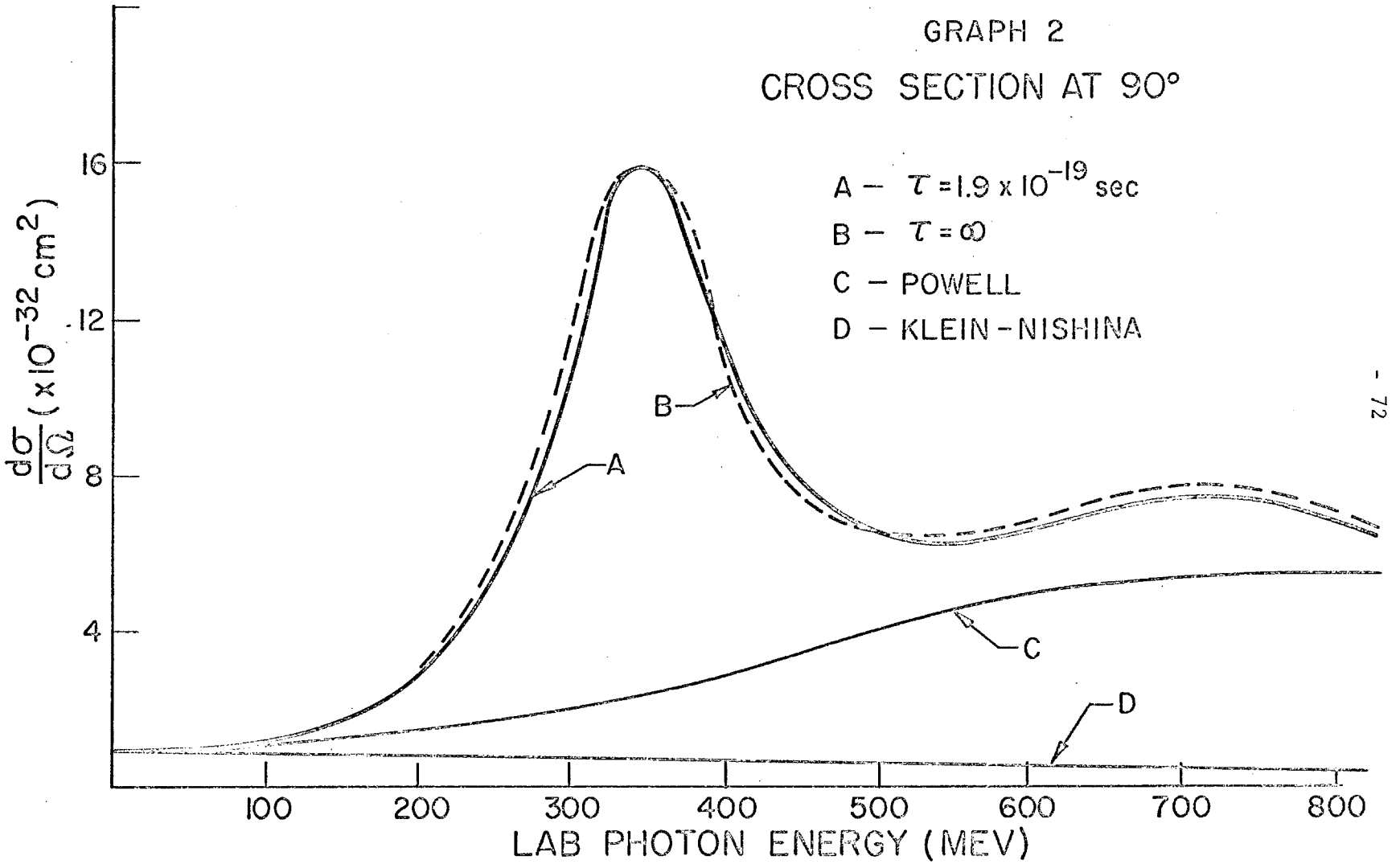
GRAPH 2
CROSS SECTION AT 90°
A – τ = 1.9 x 10^-19 sec
B – τ = ∞
C – POWELL
D – KLEIN-NISHINA
dσ/dΩ (x10^-32 cm^2)
16
12
8
4
A
B
C
D
100
200
300
400
500
600
700
800
LAB PHOTON ENERGY (MEV)

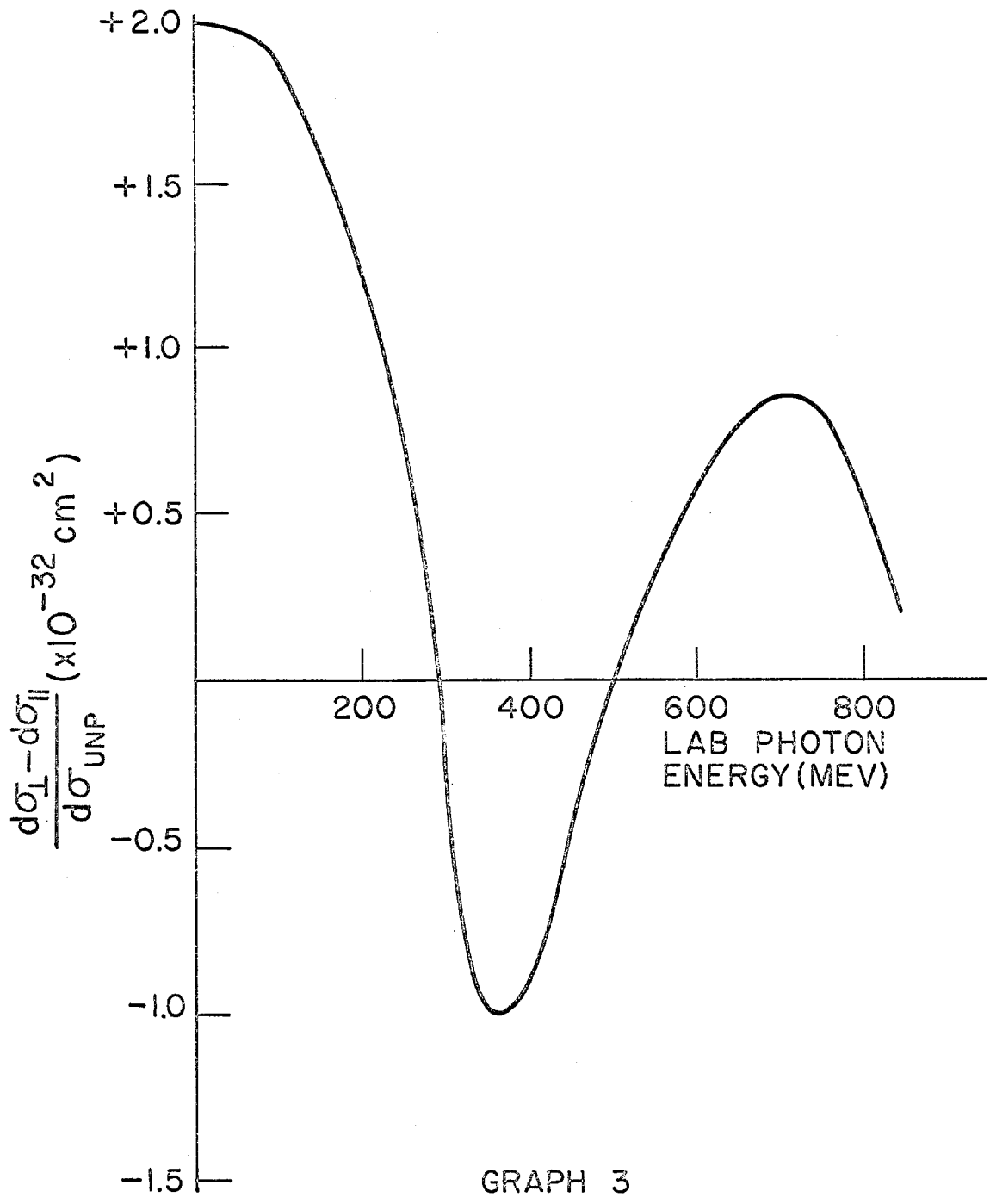

GRAPH 3

CROSS-SECTION FOR POLARIZED PHOTONS AT 90° CM

GRAPH 4

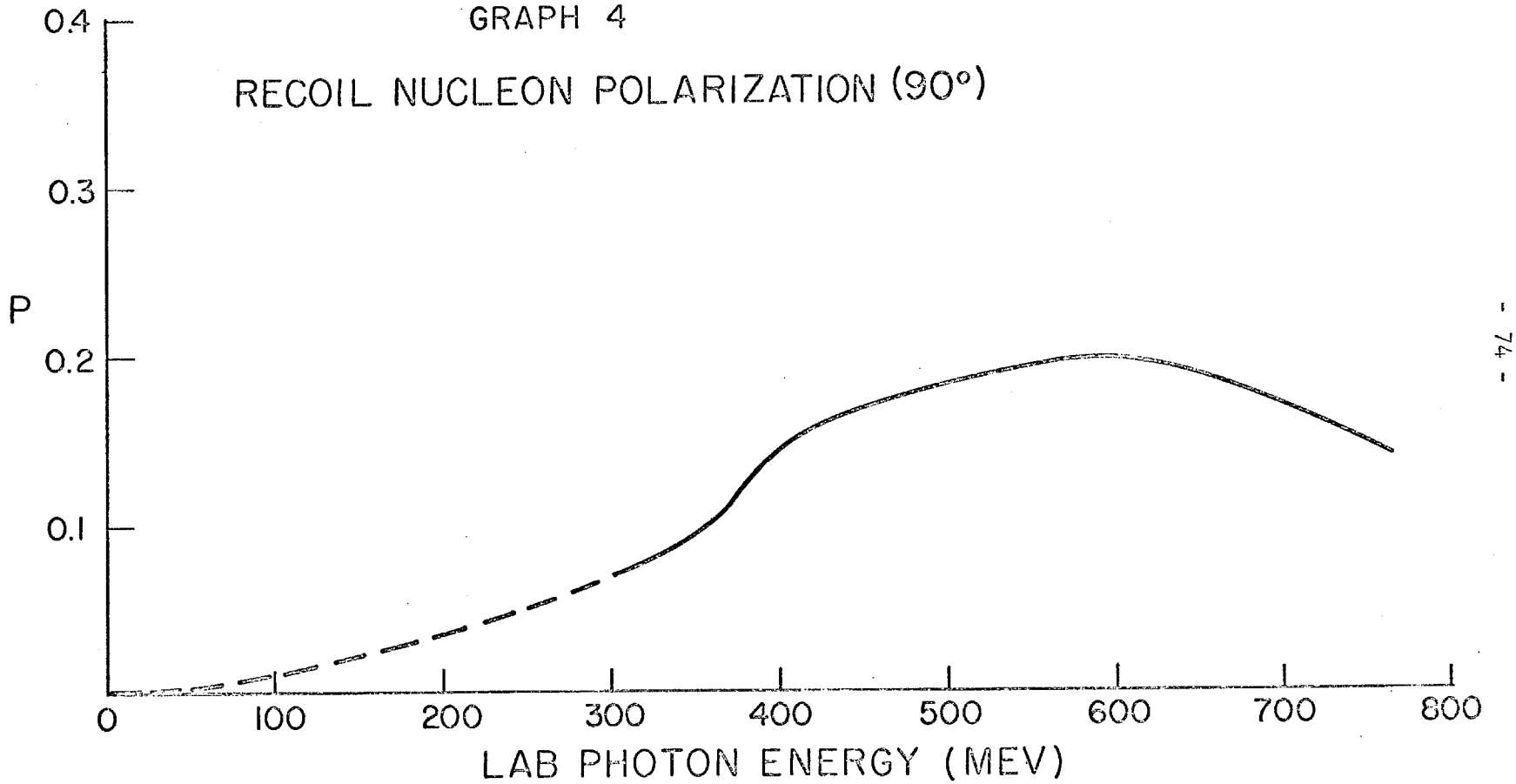
RECOIL NUCLEON POLARIZATION (90°)
P
0.4
0.3
0.2
0.1
0
100
200
300
400
500
600
700
800
LAB PHOTON ENERGY (MEV)

GRAPH 5

ANGULAR DISTRIBUTION
AT MASS OF N*

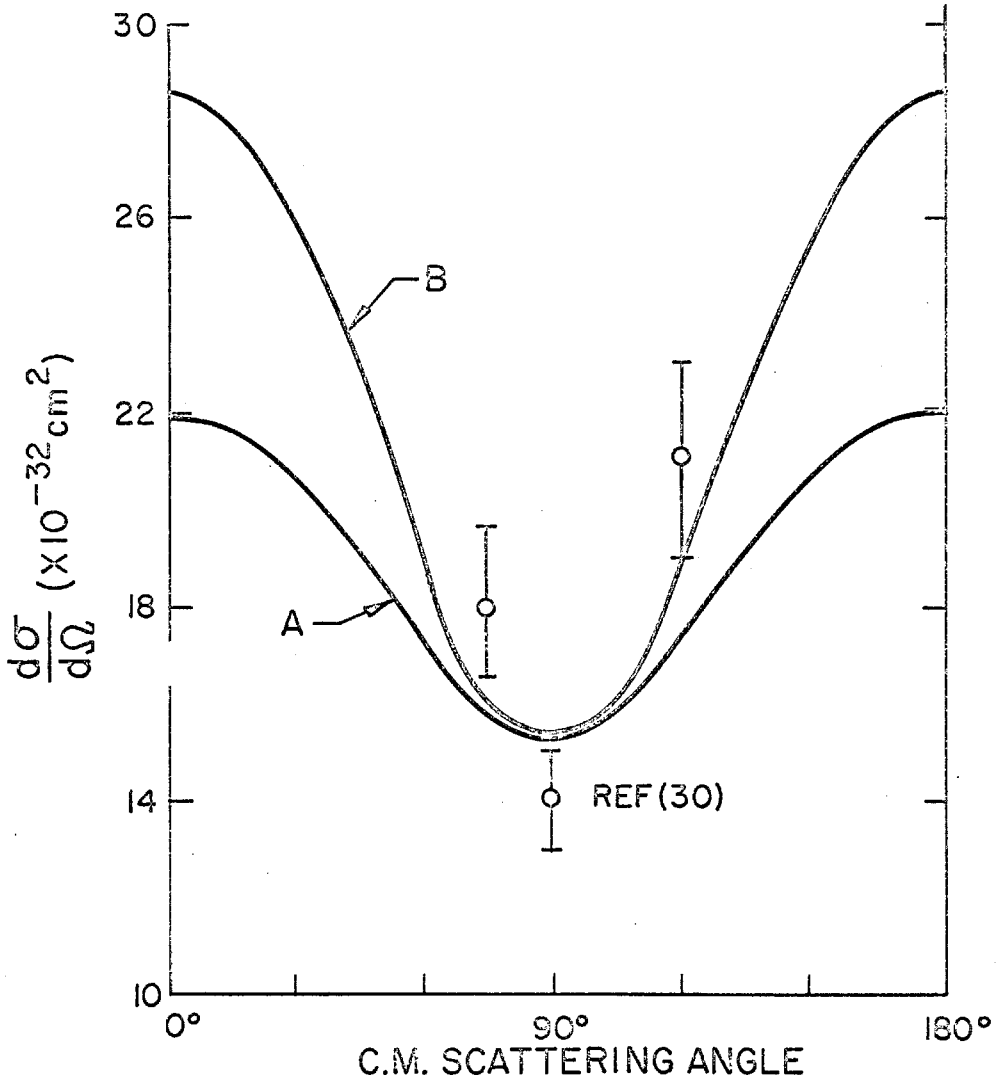

A – MAGNETIC DIPOLE
B – N* ISOBAR

REFERENCES

1. M. Gell-Mann, M.L. Goldberger and W.E. Thirring, Phys. Rev. 95, 1612 (1954).

2. J. Mathews, Ph.D. Thesis, California Institute of Technology, (unpublished).

3. M. Jacob and J. Mathews, Phys. Rev. 117, 854 (1960).

4. A.P. Contogouris, Phys. Rev. 124, 912 (1961).

5. A.P. Contogouris, Nuovo Cimento 25, 104 (1962).

6. A.C. Hearn and E. Leader, Phys. Rev. 126, 789 (1962).

7. M. Gell-Mann and M.L. Goldberger, Phys. Rev. 96, 1433 (1954); F.E. Low, Phys. Rev. 96, 1428 (1954).

8. A.C. Hearn and E. Leader, Report present to International Conference on Nucleon Structure at Stanford University, June 24-27, 1963.

9. D. Holliday, Ann. Phys. 24, 289 (1963); 319 (1963).

10. A.P. Contogouris and A. Verganelakis, Physics Letters 6, 103 (1963).

11. R.F. Stiening, E. Loh, and M. Deutsch, Phys. Rev. Letters 10, 536 (1963).

12. D. Rust et al. Phys. Rev. Letters 15, 938 (1965).

13. M. Gourdin and P. Salin, Nuovo Cimento 27, 193 (1963).

14. P. Salin, Nuovo Cimento 28, 1294 (1963).

15. M. Gourdin and P. Salin, Nuovo Cimento 27, 309 (1963).

16. M. Jacob and G.C. Wick, Ann. Phys. 7, 404 (1959).

17. N. Cabibbo, G. Da Prato, G. DeFranceschi and U. Mosco, Phys. Rev. Letters 9, 270 (1962).

18. W. Rarita and J. Schwinger, Phys. Rev. 60, 61 (1941).

19. P. Salin, Nuovo Cimento 32, 521 (1964).

20. J. Mathews, Phys. Rev. 137, B444 (1965).

21. D. Beder, Nuovo Cimento 33, 94 (1964).

22. R. Walker, personal communication.

23. F.E. Low, Proc. of 1958 Ann. Inter. Conf. on High-Energy Physics, p. 98.

24. M.L. Goldberger and S.B. Treiman, Nuovo Cimento 9, 451 (1958).

25. R.G. Glasser, N. Seeman and B. Stiller, Phys. Rev. 123, 1324 (1962).

26. L.I. Lapidus and Chou Kuang-chao, JETP 14, 210 (1962).

27. L.V. Filkov and N.F. Nelipa, Nuclear Phys. 59, 225 (1964).

28. B. Barret and G. Barton, Physics Letters 4, 16 (1963).

29. G. Bernardini, A. Hanson, A. Odian, T. Yamagata, L. Auerbach, and I. Filosofo, Nuovo Cimento 18, 1203 (1960).

30. J. Dewire, M. Feldman, V. Highland and R. Littauer, Phys. Rev. 124, 909 (1961).

31. Y. Nagashima, Progr. Theor. Phys. 33, 828 (1965).

32. G. Chew, M. Goldberger, F. Low and Y. Nambu, Phys. Rev. 106, 1345 (1957).